human T-cell leukemias (Nagel *et al.*, 2003; Przybylski *et al.*, 2005). *Bcl11b* encodes a member of the zinc-finger proteins (Avram *et al.*, 2000; Satterwhite *et al.*, 2001; Wakabayashi *et al.*, 2003a) and directly interacts with Sirt1, a member of a third class of Trichostatin-resistant deacetylase, and with the nucleosome remodeling and histone deacetylase complex, one of the major transcriptional corepressor complexes in mammalian cells (Senawong *et al.*, 2003; Cismasiu *et al.*, 2005). However, target genes or genes controlled by *Bcl11b* are not known. *Bcl11b*$^{-/-}$ mice die soon after birth, exhibiting the developmental arrest of thymocytes of the $\alpha\beta$ T-cell lineage (Wakabayashi *et al.*, 2003b). Interestingly, their thymocytes retain normal cellularity relative to wild-type littermates at the DN3 (CD4$^-$ CD8$^-$ CD25$^+$ CD44$^-$) developmental stage; however, apoptosis and low cellularity are observed at the DN4 (CD4$^-$ CD8$^-$ CD25$^-$ CD44$^-$) stage, accompanying with decrease of an antiapoptotic protein, Bcl-xL (Inoue *et al.*, 2006). At the DN4 stage, thymocytes re-enter into the cell-cycle and rapidly proliferate (Gounari *et al.*, 2001; van de Wetering *et al.*, 2002). As apoptosis has been considered as a mechanism to eliminate deleterious cells, the apoptotic phenotype of *Bcl11b*$^{-/-}$ thymocytes seems to contradict with Bcl11b as a tumor suppressor.

This article examines Bcl11b-lacking cells *in vitro* and *in vivo* to elucidate how the apoptosis conferred by Bcl11b deficiency contributes to tumor development. Here, we show growth stimulation-dependent apoptosis and Chk1 deregulation in those cells, suggesting a role of Bcl11b in the remedy for stress during DNA replication and maintenance of genomic stability.

Results

Growth suppression and apoptosis of Bcl11b-KD cells

Bcl11b knockdown (KD) lines were produced by transfecting plasmid DNA expressing two different short interfering RNA (siRNA) sequences into Jurkat cells, a human T-cell lymphoma line. Figure 1a shows Western blots of three KD cell lines derived from transfectants using one siRNA and Supplementary Figure S1 shows those of the other. Marked decrease in the Bcl11b expression was seen in KD lines (si-1, -2, -3), compared with two control cell lines (sc-1, -2) that were obtained with plasmid DNA expressing scramble RNA sequences. 3-(4,5-Dimethylthiazol-2-yl)-2,5-diphenyltetrazolium bromide (MTT) assay revealed repression of cell growth in all KD lines relative to control lines under the condition of 10% serum supplementation, whereas such difference was not observed at 5 or 1% serum concentration (Figure 1b). Analyses of apoptosis in 10% serum-supplemented KD cells displayed elevated proportions of Annexin V-positive cells (Figure 1c) and terminal deoxynucleotidyl transferase biotin-dUTP nick end labeling (TUNEL) staining-positive cells (Figure 1d). Consistently, cleavage of caspase-7 and decrease in expression of an antiapoptotic protein, Bcl-xL (Motoyama *et al.*, 1995), were detected (Figure 1a). This apoptotic phenotype is consistent with that in *Bcl11b*$^{-/-}$ mouse thymocytes (Wakabayashi *et al.*, 2003b; Inoue *et al.*, 2006) and may contrast with the current notion that apoptosis is reduced when tumor suppressor gene is lost.

We examined cell cycling after the release from double-thymidine block. At 10% serum concentration, most cells entered into S phase 6 h after the release but KD cells showed some delay in cell-cycle progression. It was noted that the number of the S phase cells was much lower in KD cells than control cells, whereas the number of sub-G1 phase cells was higher (Figure 1e). This suggests the abrogation of S phase checkpoint in KD cells and resulting apoptosis of some KD cells. On the other hand, analysis at 5% serum concentration revealed slowing down of cell-cycle progression in both KD and control cell lines. Of note is that no sub-G1 cells were detected in KD cells, indicating absence of apoptosis (Figure 1e). These results indicate that at 10% serum concentration, Bcl11b down regulation causes inhibition of cell growth owing to apoptosis and implicate the *Bcl11b* gene in S phase checkpoint.

S phase damage response

DNA replication and UV-induced DNA damages generate single-stranded DNA (ssDNA), which serves as the signal for S phase checkpoint (Zou and Elledge, 2003). We thus examined the effect on cell growth and cell cycling of KD cells after treatment with UV. We also examined effects of Camptothecin, an inhibitor of topoisomerase I and γ-ray. Camptothecin produces both ssDNA and double-stranded DNA breaks (DSBs), whereas γ-ray generates DSBs (Kastan and Bartek, 2004; Flatten *et al.*, 2005). At 10% serum concentration, UV and Camptothecin-inhibited cell growth more markedly for KD cells, whereas ionizing radiation inhibited both KD cells and control cells equally (Figure 2a). The sub-G1 fraction was increased in KD cells over control cells after UV and Camptothecin treatments whereas the levels of the increase were similar for control and KD cells when exposed to γ-rays (Figure 2b).

Cell-cycle analysis of control cells showed persistence in the number of S phase cells 3 h after UV irradiation, indicating arrest in the cell-cycle progression (Figure 2c). In contrast, a decrease of S phase cells was observed in KD cells. These indicated impaired activation of S phase checkpoint and enhanced apoptotic response in 10% serum-supplemented KD cells.

Impairment of Chk1 phosphorylation

The ssDNA damages activate ATR and its downstream checkpoint kinases, Chk1 and Chk2 (Liu *et al.*, 2000; Abraham, 2001). We thus examined these checkpoint kinases in 10% serum-supplemented KD cells before and after UV irradiation. Figure 3a shows examples of Western blotting and Figure 3b summarizes the results. Expression of Chk1 protein did not differ between control and KD cells, and UV irradiation did not affect their protein expression. However, the phosphorylation

level of Chk1 was very low in KD cells, and UV irradiation did not elevate the phosphorylation level as did in control cells. Cdc25A, a substrate of Chk1 (Zhao *et al*., 2002), showed a high expression in KD cells, indicating the inhibition of degradation owing to Chk1 impairment. On the other hand, expression and phosphorylation levels of Chk2 did not differ between KD and control cells and were not affected by UV irradiation. These results indicated Bcl11b downregulation resulting in the impairment of Chk1 phosphorylation

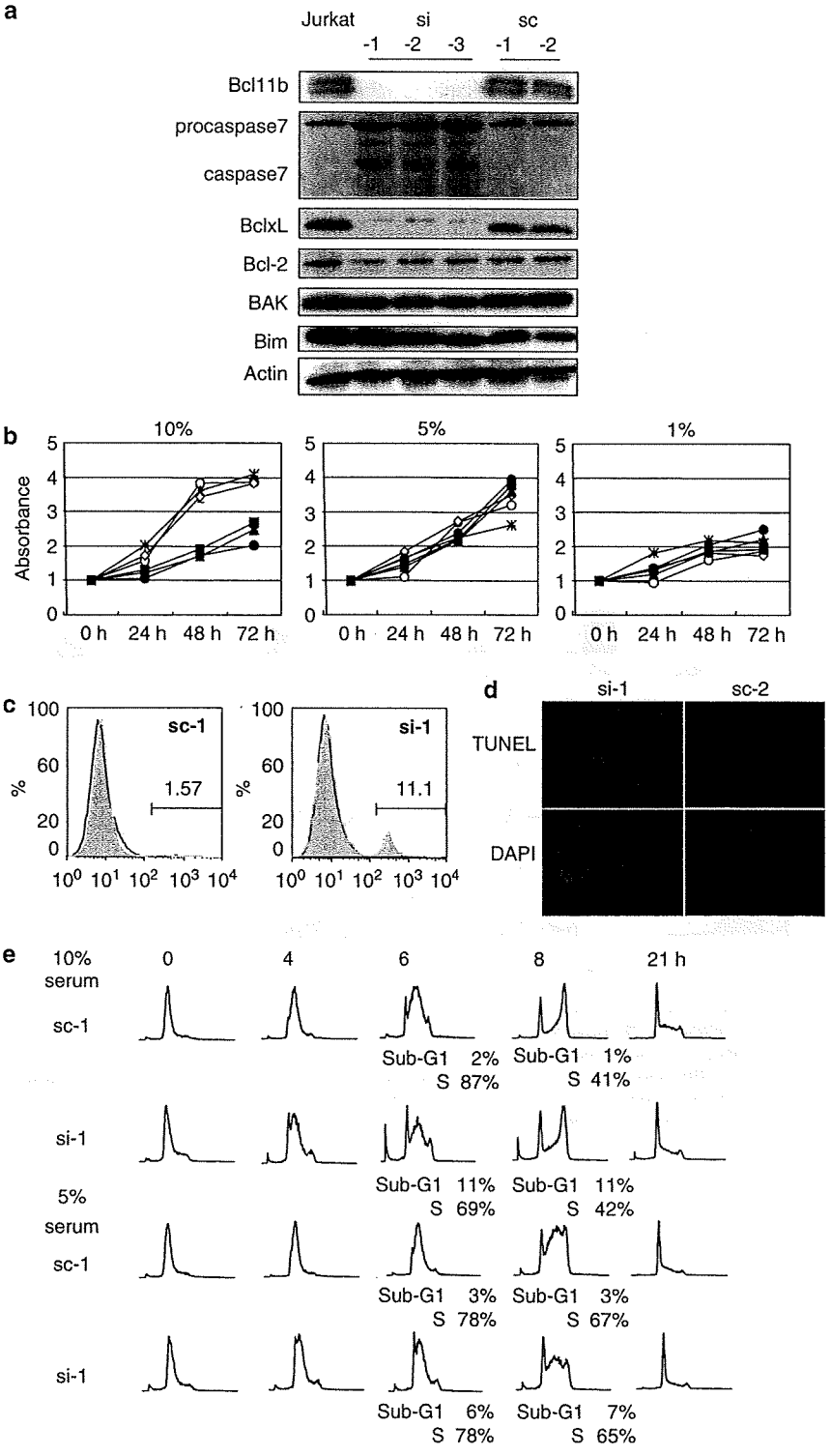

but such effect on Chk2 phosphorylation was unclear because the phosphorylation levels were not affected even in parental Jurkat or control sc-1 cells. Subcellular localization of Bcl11b and Chk1 was examined by fractionating protein extracts from Jurkat cells (Figure 3c). Most Bcl11b proteins were present in the chromatin-bound (Ch) fraction and this was not affected by UV irradiation. On the other hand, Chk1 and phosphorylated Chk1 at S317 existed in the cytoplasmic and Ch fractions. Interestingly, after UV irradiation, phosphorylated Chk1 at S317 was localized in the soluble nuclear fraction whereas phosphorylated Chk1 at S345 in the soluble nuclear and also cytoplasmic fractions. The molecular basis for this difference is not clear. These results suggest different responsiveness of Bcl11b and phosphorylated Chk1 to UV irradiation.

Chk1 phosphorylation was also examined in 5% serum-supplemented KD cells, as no difference in cell growth was observed between control and KD cells (Figure 1b). Western blot revealed no difference in the phosphorylation level between KD and control cells (Figure 3d), indicating restoration of S phase checkpoint

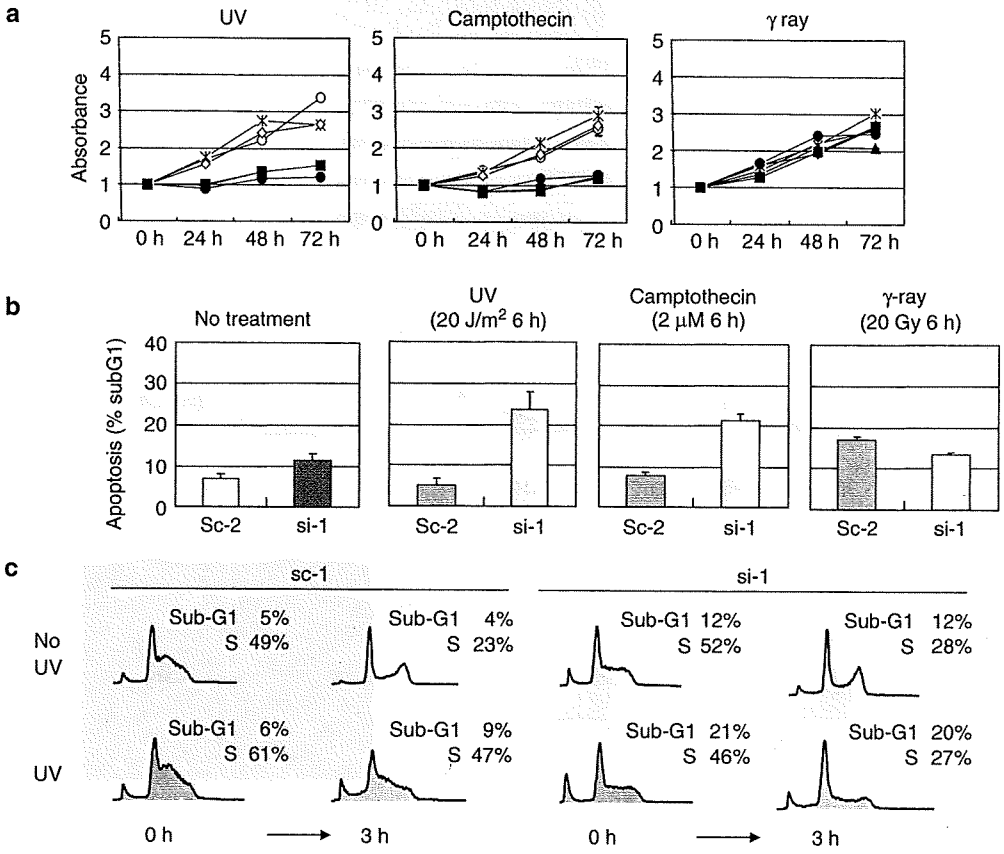

Figure 2 Impairment of S phase checkpoint. (**a**) Cell numbers shown at indicated times. The pattern of control cells is displayed in Figure 1b. Bcl11b-KD cells (closed circles, squares and triangles) are more susceptible to UV and Camptothecin than control cells (open circles, squares and triangles). That difference in susceptibility is not seen for γ-irradiation. (**b**) Summary of percents of sub-G1 phase cells in sc-2 and si-1 cells after exposure to UV, Camptothecin and γ-ray. (**c**) Cell-cycle analysis shows the abrogation of S phase checkpoint in KD cells. Six hours after the release from double thymidine block, cells were treated with UV (UV-C, 20 J/m²) and analysed with flow cytometer 3 h after. Arrest at S phase is seen in sc-1 control cells but not in si-1 cells.

Figure 1 Downregulation of *Bcl11b* inducing cell growth retardation and apoptosis. (**a**) Western blot shows cleavage of procaspase-7 and decrease in the protein level of BclxL in 10% serum-supplemented Jurkat cells when Bcl11b is downregulated by siRNA. (**b**) Cell numbers shown at indicated times: KD cells treated with siRNA (closed circles: si-1, squares: si-2 and triangles: si-3) and control cells with expression of Bcl11b (open circles: Jurkat cells, squares: sc-1 and triangles: sc-2). Bcl11b-downregulated cells show slower cell growth than control cells in the 10% serum medium but the difference disappears in the 5 or 1% serum medium. (**c**) Flow cytometric analysis of cells stained with Annexin V from indicated cell lines. The profile of normal Jurkat cells is displayed in black line. (**d**) TUNEL staining of Jurkat cells. The sc-1 and si-2 cells were treated with the TdT enzyme and stained with dUTP-fluorescein isothiocyanate using a TUNEL staining kit (Takara Inc., Japan), counterstained with 4′,6-diamidino-2-phenylindole, dihydrochloride. (**e**) Cell-cycle analysis of cells at indicated times after the release from double thymidine block. The numbers of S phase cells 6 h after the release decreases in 10% serum-supplemented KD cells whereas the numbers of sub-G1 phase cells increases. In 5% serum-supplemented cells, the number of S phase cells 8 h after the release decreases but the number of sub-G1 phase cells does not increase.

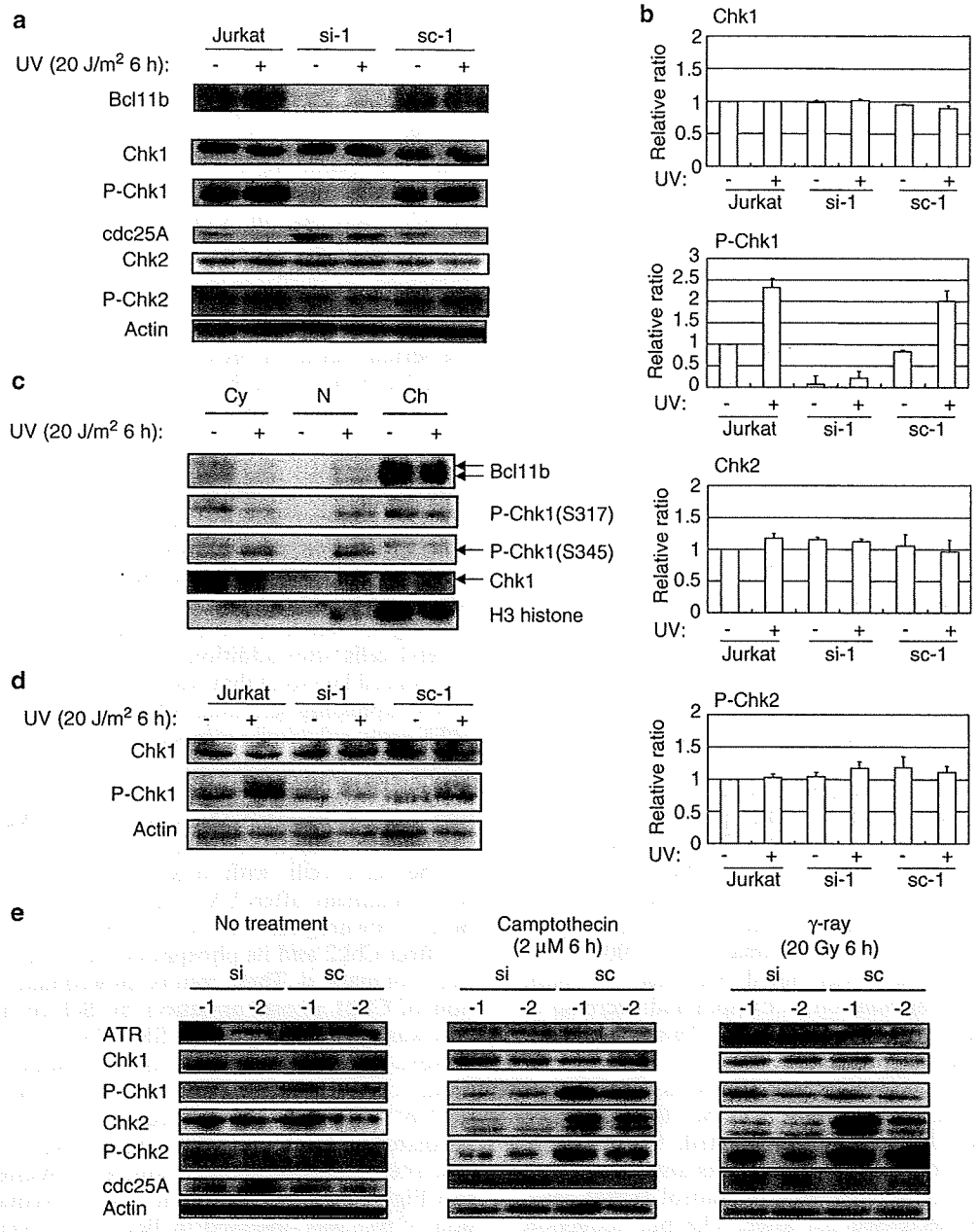

Figure 3 Effects of UV, Camptothecin and γ-ray on Chk1 and Chk2. (**a**) Western blotting of Chk1 and Chk2 proteins in 10% serum-supplemented cells. Decreased phosphorylation of Chk1 at Ser317 is seen in si-1 cells and the phosphorylation level does not increase in response to UV irradiation. Consistently, the expression of cdc25 is high in si-1 cells. No difference between control and KD cells is observed for Chk2. (**b**) Relative band ratios of Chk1, P-Chk1, Chk2 and P-Chk2 are shown, using the band intensities of β-actin as references. Results are expressed as mean and error bars show standard deviations of three independent experiments. (**c**) Subcellular localization of Bcl11b and Chk1 in Jurkat cells. Protein extracts in cytoplasmic, soluble nuclear and Ch fractions were probed with antibodies against Bcl11b, Chk1, phosphorylated Chk1 at S317 and S345 and histone H3. Bcl11b and phosphorylated Chk1 are mainly localized at the chromatin but they are differently fractionated in UV-irradiated cells. (**d**) Western blots in 5% serum-supplemented cells. The phosphorylation level of Chk1 in si-1 cells is similar to that in sc-1 cells but does not increase in response to UV irradiation. (**e**) Chk1 and Chk2 phosphorylation after exposure to Camptothecin and γ-ray. The phosphorylation level of Chk1 at Ser317 increases 6 h after administration of Camptothecin in control cells (sc-1 and sc-2) but not in KD cells (si-1 and si-2). Also, the phosphorylation level of Chk2 does not increase in si-1 and si-2 cells in response to UV irradiation. On the other hand, exposure of si-1 and si-2 cells to γ-ray affects the phosphorylation of Chk2 but not Chk1. Collectively, impairment in Chk1 phosphorylation only is seen for UV irradiation, impairment in the phosphorylation of both Chk1 and Chk2 is seen for Camptothecin treatment and impairment in Chk2 phosphorylation only is seen for γ-ray irradiation.

under this culture condition. However, UV irradiation did not increase the Chk1 phosphorylation in KD cells. This suggests that the Bcl11b-lacking state provides a latent defect in S phase checkpoint which is revealed by growth stimuli and/or UV irradiation.

Figure 3e shows effect of Camptothecin and γ-irradiation. Administration of Camptothecin in KD cells exhibited impairment of phosphorylation for both Chk1 and Chk2 probably owing to generation of ssDNA and DSBs whereas the impairment was seen only for Chk2 after γ-ray producing DSBs. The results revealed inability of Bcl11b-KD cells to activate both Chk1 and Chk2 in response to DNA-damaging agents. Among other proteins involved in ATR/Chk1 signaling pathway, expression of Claspin was found to decrease in 10% serum-supplemented KD cells (Supplementary Figure S2). As Claspin is required for activation of Chk1 by ATR (Lin *et al.*, 2004), this decrease may be relevant for reduced phosphorylation of Chk1 in KD cells.

Apoptosis, deregulated cell-cycle checkpoint and Sirt1 connection

Recently, Clarke *et al.* (2005) reported that Claspin is a specific substrate of caspase-7 and cleaved during the initiation of genotoxic stress-induced apoptosis and that the Claspin processing regulates Chk1 activity. Accordingly, the Claspin cleavage may account for our finding of impaired Chk1 phosphorylation in 10% serum-supplemented KD cells. We thus performed Western blotting of caspase-7, Claspin, Chk1 in KD cells harvested at various times after shifting from 5 to 10% serum. Also, Bcl-xL and p27 were examined, because the serum elevation triggers cell-cycle progression regulated by p27 (Nakayama *et al.*, 2004). The cleavage of caspase-7 was noted 3 h after the shift, followed by the degradation of Claspin and decrease of phosphorylated Chk1 (Figure 4a). This suggests a cascade of the activation of caspase-7, cleavage of Claspin and the inactivation of Chk1 kinase, consistent with that by Clarke *et al.* (2005). On the other hand, the amount of Bcl-xL was low to start with but markedly decreased 6 h after. p27 expression was also low in KD cells, though unexpectedly high in control Jurkat cells, and markedly decreased 3 h after. The p27 reduction probably results in a rapid G1 progression that may contribute to apoptosis under the low concentration of Bcl-xL.

Elevation of the serum concentration triggers PI3K/Akt kinase signaling and affects Sirt1 activity that associates with Bcl11b (Levine *et al.*, 2006). Thus, we examined Akt and Sirt1 by Western blotting (Figure 4b). No noticeable difference was seen in the level of Akt or phosphorylated Akt between the 10 and 5% serum concentrations. On the other hand, Sirt1 protein showed a substantial, though not marked, decrease in 10% serum-supplemented KD cells. The amount of another Bcl11b-associated protein, metastasis-associated protein 1 (Mta1) (Bagheri-Yarmand *et al.*, 2004; Cismasiu *et al.*, 2005), also decreased.

Sirt1 affects expression of a Foxo3a-target gene, *p27*, at the transcription level (Brunet *et al.*, 2004; Motta *et al.*, 2004). As Sirt1 proteins decreased in 10% serum-supplemented KD cells, we examined mRNA expression of *p27* and other genes presumably regulated by Foxo3a and Sirt1 in KD cells at various times after the serum shift. Semiquantitative reverse transcription–polymerase chain reaction (RT–PCR) showed that the mRNA level of *p27* decreased in KD cells 3 h after whereas the expression of *Bcl-xL* was low to start with and gradually decreased up to 24 h (Figure 4c). However, the levels of other possible Foxo3a-targets, *Bim* and *Gadd45*, were not affected. These suggest that growth stimulation by the serum elevation provides transcriptional repression of *p27* and *Bcl-xL* in *Bcl11b* KD cells but not in control *Bcl11b*-proficient cells.

Examination of cell line specificity

To test whether the Chk1 activation by Bcl11b is cell-line specific, we produced the FRSK skin keratinocyte cell line (tet-1) that expressed Bcl11b siRNA driven by a tetracycline/doxycycline inducible promoter. Western blotting showed a decrease in the expression of Bcl11b in tet-1 cells after addition of doxycycline but not in a control cell line (c-1) that was obtained by using plasmid DNA expressing scramble RNA sequences (Figure 5a). MTT assay exhibited repression of cell growth in the tet-1 cells in the presence of doxycycline (open circles) (Figure 5b). UV irradiation enhanced the growth repression, as in Bcl11b-KD Jurkat cells. Western blots showed a minimal decrease in Chk1 phosphorylation in the tet-1 cells with doxycycline but the decrease was prominent after UV irradiation (Figure 5a). The Bcl11b downregulation and UV irradiation also seemed to affect Chk2 and its phosphorylation but those effects were not marked. These results showed that the suppression of Chk1 phosphorylation by Bcl11b downregulation was also detected in FRSK cells.

Next, we examined mouse thymocytes *in vivo*. Thymocytes isolated from *Bcl11b*$^{+/+}$, *Bcl11b*$^{+/-}$ and *Bcl11b*$^{-/-}$ mice were incubated in the culture medium, irradiated with UV and examined for protein expression 18 h after. Figure 6a shows examples of Western blotting and Figure 6b summarizes the results. Reduced expression of p27 was observed in Bcl11b$^{-/-}$ thymocytes and the expression was restored to the control level by UV irradiation. The cleavage of Claspin was seen in Bcl11b$^{-/-}$ thymocytes and was enhanced by UV irradiation. On the other hand, protein levels of Chk1 or Chk2 did not differ in thymocytes between the three different *Bcl11b* genotypes, nor were they affected by UV irradiation. However, Bcl11b deficiency reduced phosphorylation of Chk1 at the S317 and S345 positions and also phosphorylation of Chk2. In addition, UV-induced phosphorylation of Chk1 much less in *Bcl11b*$^{-/-}$ thymocytes than in control thymocytes. Fivefold amount of protein extracts from irradiated *Bcl11b*$^{-/-}$ thymocytes allowed us to detect phospholylated Chk1. On the other hand, UV irradiation-induced phosphorylation of Chk2 in thymocytes of all the three different genotypes. p53

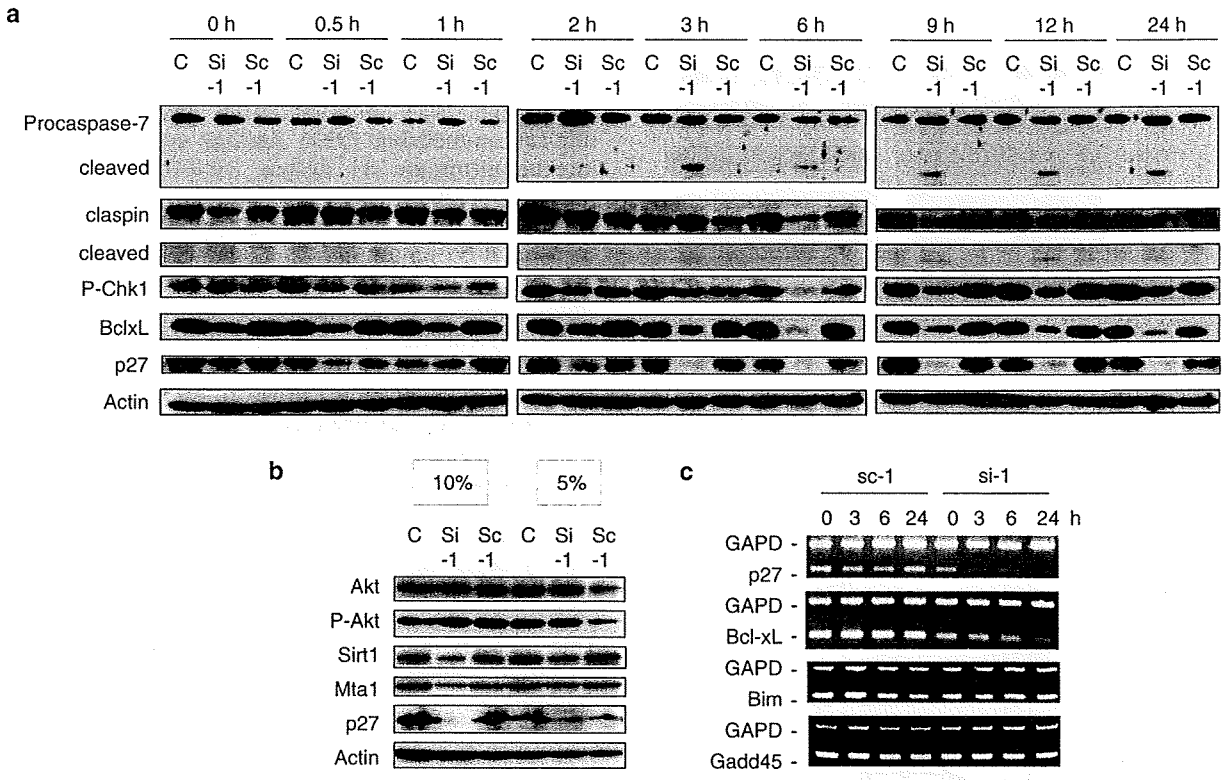

Figure 4 Changes of various proteins and RNA in Bcl11b-KD cells after growth stimulation. (**a**) Western blots of cells harvested at indicated times after changing the medium containing 5%–10% serum. Cleavage of procaspase-7 is noted 3 h after the change, and decreases in Claspin and phosphorylated Chk1 at Ser317 are seen 6 h after. Bcl-xL is low at the beginning and markedly decreases 3–6 h after and p27 decrease starts at 2 h after. (**b**) Western blots of Akt, Sirt1, Mta1 and p27 in 10 and 5% serum-supplemented cells. Expression or phosphorylation level of Akt on the mammalian target of rapamycin signaling pathway does not change. Expression levels of Sirt1, Mta1 and p27 proteins are lower in si-1 cells than sc-1 cells in the medium containing 10% serum. The difference is much less in that containing 5% serum. (**c**) RT–PCR analysis of cells harvested at indicated times after the medium change. The mRNA amount of *p27* rapidly decreases 3 h after whereas that of *Bcl-xL* is low at the beginning and gradually decreases until 24 h after. No change is seen in *Bim* or *Gadd45* mRNAs.

proteins in Bcl11b$^{-/-}$ thymocytes increased in response to UV irradiation. These results indicate that Bcl11b downregulation or deficiency leads to decrease of p27 and suppression of Chk1 phosphorylation both *in vitro* and *in vivo*.

Discussion

This paper shows that Bcl11b-KD T-cell lines, when exposed to growth stimuli or UV radiation, exhibited extensive apoptosis with concomitant decreases in p27 and Bcl-xL. Also, deregulation of Chk1 phosphorylation was observed in the KD cells and *Bcl11b*$^{-/-}$ thymocytes after UV irradiation. These implicate Bcl11b in resisting DNA replication stress or DNA damages, although it is not clear how Bcl11b remedies these stresses. Bcl11b directly interacts with Sirt1 deacetylase (Senawong *et al.*, 2003), and hence the Bcl11b deficiency may affect some Sirt1 activity. In fact, the amount of Sirt1 decreased in Bcl1b-KD cells relative to parental Jurkat cells where most Bcl11b proteins were localized at the chromatin. Sirt1 downregulates Foxo transcription factors but does not regulate all Foxo target genes in the same manner in different cellular contexts, because target genes such as *p27* and *Gadd45* are upregulated by Sirt1 in Foxo3a-expressing fibroblasts whereas another target of *Bim* gene is not affected (Brunet *et al.*, 2004; Motta *et al.*, 2004). Similar differential regulation was observed for Bcl11b in Jurkat cells. In 10% serum-supplemented Bcl11b-KD cells, *p27* expression decreased whereas expression of *Bim* or *Gadd45* was not affected. In addition, decreased expression of *Bcl-xL* was observed in those cells. Therefore, Bcl11b may affect a subset of Foxo target genes through Sirt1 activity, and these affected genes overlap with but are different from those of Sirt1 in the absence of Bcl11b. Activity of the Foxo factors is not only regulated through acetylation but also through phosphorylation by Akt (Levine *et al.*, 2006). However, this possibility is less likely in KD cells because the phosphorylation level of Akt did not increase in response to growth factor activation. Collectively, decreases in p27 and Bcl-xL might account for all the enhanced apoptosis associated with Bcl11b deficiency.

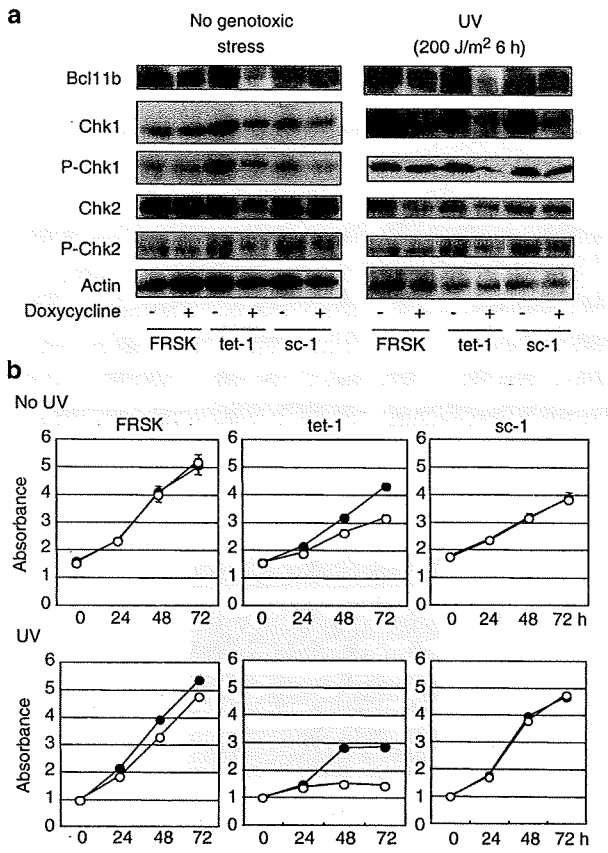

Figure 5 Bcl11b downregulation inhibits Chk1 phosphorylation in a keratinocyte cell line. (**a**) Western blot shows a decrease in the Bcl11b expression in tet-1 cells when doxycycline is added. The tet-1 cells under the presence of doxycycline phosphorylated Chk1 after UV irradiation much less than control cells. (**b**) The cell number is shown. In the presence of doxycycline (open circles), tet-1 cells, but not control c-1 cells, show slower cell growth than cells in the absence of doxycycline (closed circles). The difference in cell growth was prominent when UV and Camptothecin were treated.

Apoptosis has been considered as a mechanism to eliminate deleterious cells with DNA damages and hence apoptotic phenotype of the KD cells and *Bcl11b*$^{-/-}$ thymocytes seems to contradict with Bcl11b as a tumor suppressor. However, hyperplastic or dysplastic cells often exhibit apoptotic phenotype together with high mitotic index (Bartkova *et al.*, 2005; Gorgoulis *et al.*, 2005). Therefore, the apoptotic phenotype may be a reflection of accumulation of DNA damages or a deregulated elevation in cell-cycle progression in those cells. Such precancerous cells probably develop a rapidly progressive tumor phenotype when they acquire the ability to escape apoptosis. Our preliminary analysis showed that apoptosiS prone Bcl11b-deficient cells are capable to develop tumors, as transfer of *Bcl11b*$^{-/-}$ fetal liver cells into severe combined immunodeficiency mice led to the development of lymphomas at a frequency of four out of 12 cases (data not shown). On the other hand, the present study suggests a concealed function of apoptosis, which positively contributes to tumorigenesis. The activation of caspase-7 resulted in the Claspin cleavage which downregulated phosphorylation of Chk1, consistent with the previous report (Clarke *et al.*, 2005). This deregulation of Chk1 leading to a high level of Cdc25A is likely to enhance replication-mediated DNA damage accumulation during inappropriate cell cycling, contributing to tumor progression (Walworth *et al.*, 1993; Sanchez *et al.*, 1997; Takai *et al.*, 2000; Lam *et al.*, 2004). A second possible consequence of apoptosis is a generation of chromosomal translocations through DSBs caused by apoptotic endonucleases, as exemplified in *Tel-AML1* translocations (Eguchi-Ishimae *et al.* 2001). These possibilities may be supported by that selective components of the apoptotic process can be activated, followed by recovery of a normal cellular phenotype in the absence of apoptotic morphology (Alam *et al.*, 1999; Hoeppner *et al.*, 2001; Reddien *et al.*, 2001).

Finally, it is known that Chk1 downregulation potentiates antimetabolites and topoisomerase inhibitors by depriving the cancer cells of the Chk1 defensive mechanism (Zhou and Bartek, 2004). Likewise, Bcl11b downregulation sensitizes Jurkat cells to Camptothecin. This suggests that not only Chk1 but also Bcl11b is a potential application target of inhibitors in cancer therapy.

Materials and methods

Mice and genotyping

Bcl11b$^{+/-}$ mice of BALB/c background used in this study were maintained under specific pathogen-free conditions in the animal colony of the Niigata University. *Bcl11b*$^{-/-}$ mice were obtained by mating *Bcl11b*$^{+/-}$ mice. Isolation of genomic DNA from brain and thymic lymphomas was carried out by standard protocols. Genotyping of *Bcl11b* was carried out as described previously (Wakabayashi *et al.*, 2003a; Sakata *et al.*, 2004). All animal experiments comply to the guidelines by the animal ethics committee for animal experimentation of Niigata University.

Cells

Jurkat cells (p53 deficient) were cultured in Roswell Park Memorial Institute 1640 medium (Sigma, St Louis, MO, USA) containing 10% fetal bovine serum and 100 U/ml penicillin and streptomycin. Two different fragments of 64 nucleotides for siRNA covering the nucleotide positions 646–667 and 1303–1324 (see the Supplementary Figure S2 legend) of human Bcl11b coding region and scramble 21nt-sequence were cloned into pSilencer 2.1-U6 neo (Ambion, Austin, TX, USA). These vectors were transfected into Jurkat cells using DMRIE-C followed by G418 selection. Three and two independent clones (si-1, -2 -3 and si-a, -b) were isolated from the 646–667 region and the 1303–1324 region, respectively, and used. As for the FRSK cells (p53 deficient), the tet-on operator was incorporated into the pSilencer 2.1-U6 neo clone, and this was co-transfected with a hygromycin marker. One of the three independent hygromycin-resistant clones was selected, which showed low spontaneous expression but high inducibility of siRNA expression upon treatment with doxycycline at the dose of 5 μg/ml. The tet-inducible FRSK cells were cultured in the medium containing 10% tet-approved fetal bovine serum

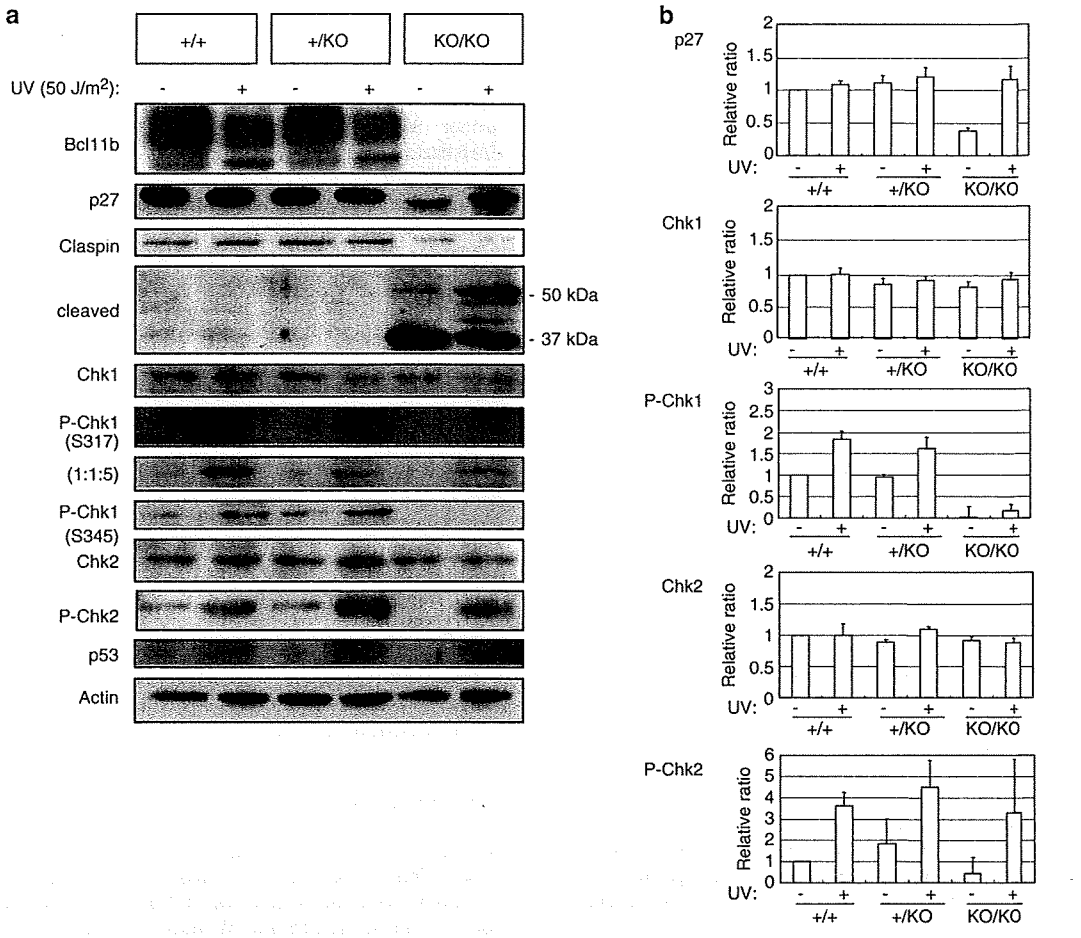

Figure 6 Deregulation of Chk1, but not Chk2, in *Bcl11b*$^{-/-}$ thymocytes. (**a**) Western blots show p27 reduction, degradation of Claspin and impairment of Chk1 phosphorylation at Ser317 and at Ser345 in *Bcl11b*$^{-/-}$ thymocytes. Increase in phosphorylation of Chk1 in response to UV irradiation is much less in *Bcl11b*$^{-/-}$ thymocytes than in *Bcl11b*$^{+/-}$ and *Bcl11b*$^{+/+}$ thymocytes. Fivefold amount of *Bcl11b*$^{-/-}$ thymocyte extracts provides a visible band of phospholylated Chk1. On the other hand, UV inducibility of phosphorylated Chk2 and p53 proteins is detected in *Bcl11b*$^{-/-}$ thymocytes. (**b**) Relative band ratios of p27, Chk1, P-Chk1, Chk2 and P-Chk2 are shown, using the band intensities of β-actin as references. Results are expressed as mean and error bars show standard deviations of three independent experiments.

(Clontech, Mountain View, CA, USA), 100 μg/ml of G418 and 50 μg/ml of hygromycin.

MTT cell growth assay

Jurkat cells were plated in 96-well tissue culture dishes at 5×10^4 cells per well in 100 μl of the medium and treated with and without UV, Camptothecin, or γ-ray. FRSK cells were treated in a similar manner in the medium containing doxycycline and in the medium without doxycycline. MTT reagents were added to the cells at the indicated times after the treatment, followed by counting with Premix WST-1 Cell Proliferation Assay System (Takara Inc., Kyoto, Japan).

Synchronization of cells and cell-cycle

Jurkat cells were incubated in the medium containing 0.56 mM thymidine (Sigma) for 18 h. After cultured for 15 h in thymidine-free medium, the cells were again incubated in the same medium for 15 h. Those cells were used for assays after the medium was removed. Six hours after the removal, cells were treated with UV and further incubated for indicated times. After washed in phosphate-buffered saline (PBS) and fixed in 70% ethanol, the cells were stained with propidium iodide, and subjected to analyses by FACSscan flow cytometer (BD Bioscience, San Jose, CA, USA), as described previously (Wakabayashi *et al*., 2003b).

Detections of apoptosis

Apoptosis was analysed using Annexin V (BD Biosciences Clontech, Mountain View, CA, USA) by FACSscan flow cytometer (Becton Dickinson) according to the manufacture's protocol.

Fractionation into subcellular components

Jurkat cells were suspended in a buffer containing 0.2% NP-40 and fractionated as described (Andegeko *et al*., 2001). Cytoplasmic fraction (Cy) was separated from nuclei by low-speed centrifugation, and the isolated nuclei were resuspended in the buffer containing 0.5% NP-40 and subjected to high-speed centrifugation to obtain soluble nuclear (N) and chromatin-bound (Ch) fractions. The proteins in each fraction

were separated by sodium dodecyl sulfate–polyacrylamide gel electrophoresis (SDS–PAGE) and duplicate membranes were blotted with antibodies against Bcl11b, Chk1, phosphorylated Chk1 at S317 and at S345 and histone H3.

Western blotting

Thymocytes and culture cells were suspended in PBS and mixed with an equal volume of lysis buffer, 0.125 M Tris–HCl (pH 6.8), 10% sucrose, 10% SDS, 10% 2-ME and 0.004% bromophenol blue. The extract was electrophoresed in 8 and 14% SDS–PAGE gels and blotted onto Hybond membranes (Amersham Pharmacia Biotech, Piscataway, NJ, USA). Antibodies used are listed below. Protein bands were visualized using chemiluminescent detection (ECL plus, Amersham Pharmacia Biotech).

Antibodies

Rabbit anti-Bcl11b-Z antibodies used in these experiments have been described previously (Wakabayashi *et al*., 2003b). Anti-caspase-7 (no. 9492), anti-Bcl-xL (no. 2762), anti-p27 Kip1 (no. 2552), anti-Akt (no. 9272), anti-Akt(pSer473) (no. 9271), anti-Chk1 (no. 2345), anti-Chk1(pSer317) (#2344), anti-Chk1(pSer345) (no. 2341), anti-Chk2 (no. 2662), anti-Chk2 (pThr68) (#2661), anti-cdc25A (no. 3652), anti-cdc25C (no. 922), anti-cdc25C(p216) (no. 9528), anti-ATR(pSer428) (no. 2853) and anti-p53 (no. 9282) were purchased from Cell Signaling Technology (Beverly, MA, USA). Anti-ATR (no. sc-1887), antiactin (no. sc-1615), anti-claspin (no. sc-27297), anti-BRCA1 (no. sc-6954), anti-Rad50 (no. sc-20155), anti-Rad9 (no. sc-10465), anti-Rad1 (no. sc-14314), anti-Hus1 (no. sc-8323), anti-MRE11 (no. sc-5859), anti-GADD45(#sc-797), anti-MTA1 (#sc-26654), anti-SIRT1 (no. sc-15404) and horse raddish peroxidase (HRP)-anti-goat immunoglobulin G (IgG) (#sc-2020) were purchased from Santa Cruz Biotechnology (Santa Cruz, CA, USA). Anti-NBS1 (#A300-187A) was purchased from Bethyl Laboratories (Montgomery, TX, USA). HRP-anti-rabbit IgG (no. NA934V) was purchased from Amersham Pharmacia Biotech.

RT–PCR

Total RNA was prepared from Jurkat cells using the RNA Easy Mini kit (Quiagen, Valencia, CA, USA) according to the protocol recommended by the manufacturer. cDNA was synthesized from 1–5 μg of total RNA with an oligo(dT) primer using SuperScript II reverse transcriptase (Invitrogen, Carlsbad, CA, USA) and an aliquot (1–2 of cDNA products) was used for PCR using primers listed below. Multiplex PCR was carried out similarly where glyceraldehyde-3-phosphate dehydrogenase (GAPDH) primers were always included as a reference. PCR products were separated by electrophoresis in 1% agarose gel and visualized by staining with ethidium bromide.

The primers used in RT–PCR was followed:

GAPDH(forward): GGTCGGAGTCAACGGATTTGGTCG;
GAPDH(reverse): CCTCCGACGCCTGCTTCACCAC;
p27(forward): TTGCCCGAGTTCTACTACAGACCCC;
p27(reverse): CGAGCTGTTTACGTTTGACG;
BclxL(forward): ATGAACTCTTCCGGGATGG;
BclxL(reverse): TGGATCCAAGGCTCTAGGTG;
BIM(forward): TCCCTACAGACAGAGCCACAAGGT;
BIM(reverse): CAGGTTCAGCCTGCCTCATGGAAG;
GADD45(forward): ACGAGGACGACGACAGAGAT;
GADD45(reverse): GCAGGATCCTTCCATTGAGA.

The PCR program was: 10 min at 94°C, followed by 25 cycles (30 s at 94°C, 30 s at 54°C, 1 min at 72°C), followed by 7 min extension at 72°C.

Acknowledgements

We thank O Niwa and A Balmain for helpful comments on the paper. This work was supported by grants-in-aid for Cancer Research from the Ministries of Education, Science, Art and Sports, and of Health and Welfare of Japan.

References

Andegeko Y, Moyal L, Mittelman L, Tsarfaty I, Shiloh Y. (2001). Nuclear retention of ATM at sites of DNA double strand breaks. *J Biol Chem* **276**: 38224–38230.

Abraham RT. (2001). Cell-cycle checkpoint signaling through the ATM and ATR kinases. *Genes Dev* **15**: 2177–2196.

Alam A, Cohen LY, Aouad S, Sekaly RP. (1999). Early activation of caspases during T lymphocyte stimulation results in selective substrate cleavage in nonapoptotic cells. *J Exp Med* **190**: 1879–1890.

Avram D, Fields A, Pretty On Top K, Nevrivy DJ, Ishmael JE, Leid M. (2000). Isolation of a novel family of C2H2 zinc finger proteins implicated in transcriptional repression mediated by chicken ovalbumin upstream promoter transcription factor (COUP-TF) orphan nuclear receptors. *J Biol Chem* **275**: 10315–10322.

Bagheri-Yarmand R, Talukder AH, Wang RA, Vadlamudi RK, Kumar R. (2004). Metastasis-associated protein 1 deregulation causes inappropriate mammary gland development and tumorigenesis. *Development* **131**: 3469–3479.

Bartkova J, Horejsi Z, Koed K, Kramer A, Tort F, Zieger K *et al*. (2005). DNA damage response as a candidate anti-cancer barrier in early human tumorigenesis. *Nature* **434**: 864–870.

Brunet A, Sweeney LB, Sturgill JF, Chua KF, Greer PL, Lin Y *et al*. (2004). Stress-dependent regulation of FOXO transcription factors by the SIRT1 deacetylase. *Science* **303**: 2011–2015.

Chen Y, Sanchez Y. (2004). Chk1 in the DNA damage response: conserved roles from yeasts to mammals. *DNA Repair (Amst)* **3**: 1025–1032.

Cismasiu VB, Adamo K, Gecewicz J, Duque J, Lin Q, Avram D. (2005). BCL11B functionally associates with the NuRD complex in T lymphocytes to repress targeted promoter. *Oncogene* **24**: 6753–6764.

Clarke CA, Bennett LN, Clarke PR. (2005). Cleavage of Claspin by caspase-7 during apoptosis inhibits the Chk1 pathway. *J Biol Chem* **280**: 35337–35345.

Di Cristofano A, De Acetis M, Koff A, Cordon-Cardo C, Pandolfi PP. (2001). Pten and p27^{KIP1} cooperate in prostate cancer tumor suppression in the mouse. *Nat Genet* **27**: 222–224.

Eguchi-Ishimae M, Eguchi M, Ishii E, Miyazaki S, Ueda K, Kamada N *et al*. (2001). Breakage and fusion of the TEL (ETV6) gene in immature B lymphocytes induced by apoptogenic signals. *Blood* **97**: 737–743.

Fero ML, Randel E, Gurley KE, Roberts JM, Kemp CJ. (1998). The murine gene p27^{Kip1} is haplo-insufficient for tumor suppression. *Nature* **396**: 177–180.

Fero ML, Rivkin M, Tasch M, Porter P, Carow CE, Firpo E *et al*. (1996). A syndrome of multiorgan hyperplasia with

features of gigantism, tumorigenesis, and female sterility in p27(Kip1)-deficient mice. *Cell* **85**: 733–744.

Flatten K, Dai N, Vroman BT, Loegering D, Erlichman C, Karnitz LM *et al.* (2005). The role of checkpoint kinase 1 in sensitivity to topoisomerase I poisons. *J Biol Chem* **280**: 14349–14355.

Gorgoulis VG, Vassiliou LV, Karakaidos P, Zacharatos P, Kotsinas A, Liloglou T *et al.* (2005). Activation of the DNA damage checkpoint and genomic instability in human precancerous lesions. *Nature* **434**: 907–913.

Gounari F, Aifantis I, Khazaie K, Hoeflinger S, Harad N, Taketo MM *et al.* (2001). Somatic activation of β-catenin bypasses pre-TCR signaling and TCR selection in thymocyte development. *Nat Immunol* **2**: 863–969.

Hoeppner DJ, Hengartner MO, Schnabel R. (2001). Engulfment genes cooperate with ced-3 to promote cell death in *Caenorhabditis elegans*. *Nature* **412**: 202–206.

Inoue J, Kanefuji T, Okazuka K, Watanabe H, Mishima Y, Kominami R. (2006). Expression of TCRαβ partly rescues developmental arrest and apoptosis of αβT cells in Bcl11b$^{-/-}$ mice. *J Immunol* **176**: 5871–5879.

Kastan MB, Bartek J. (2004). Cell-cycle checkpoints and cancer. *Nature* **432**: 316–323.

Kiyokawa H, Kineman RD, Manova-Todorova KO, Soares VC, Hoffman ES, Ono M *et al.* (1996). Enhanced growth of mice lacking the cyclin-dependent kinase inhibitor function of p27(Kip1). *Cell* **85**: 721–732.

Lam MH, Liu Q, Elledge SJ, Rosen JM. (2004). Chk1 is haploinsufficient for multiple functions critical to tumor suppression. *Cancer Cell* **6**: 45–59.

Levine AJ, Feng Z, Mak TW, You H, Jin S. (2006). Coordination and communication between the p53 and IGF-1-AKT-TOR signal transduction pathways. *Genes Dev* **20**: 267–275.

Lin SY, Li K, Stewart GS, Elledge SJ. (2004). Human Claspin works with BRCA1 to both positively and negatively regulate cell proliferation. *Proc Natl Acad Sci USA* **101**: 6484–6489.

Liu Q, Guntuku S, Cui XS, Matsuoka S, Cortez D, Tamai K *et al.* (2000). Chk1 is an essential kinase that is regulated by Atr and required for the G(2)/M DNA damage checkpoint. *Genes Dev* **14**: 1448–1459.

Motoyama N, Wang F, Roth KA, Sawa H, Nakayama K, Nakayama K *et al.* (1995). Massive cell death of immature hematopoietic cells and neurons in Bcl-x-deficient mice. *Science* **267**: 1506–1510.

Motta MC, Divecha N, Lemieux M, Kamel C, Chen D, Gu W *et al.* (2004). Mammalian SIRT1 represses forkhead transcription factors. *Cell* **116**: 551–563.

Nagel S, Kaufmann M, Drexler HG, MacLeod RA. (2003). The cardiac homeobox gene NKX2-5 is deregulated by juxtaposition with BCL11B in pediatric T-ALL cell lines via a novel t(5;14)(q35.1q32.2). *Cancer Res* **63**: 5329–5334.

Nakayama K, Ishida N, Shirane M, Inomata A, Inoue T, Shishido N *et al.* (1996). Mice lacking p27(Kip1) display increased body size, multiple organ hyperplasia, retinal dysplasia, and pituitary tumors. *Cell* **85**: 707–720.

Nakayama K, Nagahama H, Minamishima YA, Miyake S, Ishida N, Hatakeyama S *et al.* (2004). Skp2-mediated degradation of p27 regulates progression into mitosis. *Dev Cell* **6**: 661–672.

Przybylski GK, Dik WA, Wanzeck J, Grabarczyk P, Majunke S, Martin-Subero JI *et al.* (2005). Disruption of the BCL11B gene through inv(14)(q11.2q32.31) results in the expression of BCL11B-TRDC fusion transcripts and is associated with the absence of wild-type BCL11B transcripts in T-ALL. *Leukemia* **19**: 201–208.

Reddien PW, Cameron S, Horvitz HR. (2001). Phagocytosis promotes programmed cell death in *C*elegans. *Nature* **412**: 198–202.

Sakata J, Inoue J, Ohi H, Kosugi-Okano H, Mishima Y, Hatakeyama K *et al.* (2004). Involvement of V(D)J recombinase in the generation of intragenic deletions in the Bcl11b/Bcl11b tumor suppressor gene in γ-ray-induced thymic lymphomas and in normal thymus of the mouse. *Carcinogenesis* **25**: 1069–1075.

Sanchez Y, Wong C, Thoma RS, Richman R, Wu Z, Piwnica-Worms H *et al.* (1997). Conservation of the Chk1 checkpoint pathway in mammals: linkage of DNA damage to Cdk regulation through Cdc25. *Science* **277**: 1497–1501.

Satterwhite E, Sonoki T, Willis TG, Harder L, Nowak R, Arriola EL *et al.* (2001). The BCL11 gene family: involvement of BCL11A in lymphoid malignancies. *Blood* **98**: 3413–3420.

Senawong T, Peterson VJ, Avram D, Shepherd DM, Frye RA, Minucci S *et al.* (2003). Involvement of the histone deacetylase SIRT1 in chicken ovalbumin upstream promoter transcription factor (COUP-TF)-interacting protein 2-mediated transcriptional repression. *J Biol Chem* **278**: 43041–43050.

Shinbo T, Matsuki A, Matsumoto Y, Kosugi S, Takahashi H, Niwa O *et al.* (1999). Allelic loss mapping and physical delineation of a region harboring a putative thymic lymphoma gene on chromosome 12. *Oncogene* **12**: 4131–4136.

Takai H, Tominaga K, Motoyama N, Minamishima YA, Nagahama H, Tsukiyama T *et al.* (2000). Aberrant cell-cycle checkpoint function and early embryonic death in Chk1(−/−) mice. *Genes Dev* **14**: 1439–1447.

van de Wetering M, de Lau W, Clevers H. (2002). WNT signaling and lymphocyte development. *Cell* **109**: S13–S19.

Wakabayashi Y, Inoue J, Takahashi Y, Matsuki A, Kosugi-Okano H, Shinbo T *et al.* (2003a). Homozygous deletions and point mutations of the Bcl11b/Bcl11b gene in γ-ray induced mouse thymic lymphomas. *Biochem Biophys Res Commun* **301**: 598–603.

Wakabayashi Y, Watanabe H, Inoue J, Takeda N, Sakata J, Mishima Y *et al.* (2003b). Bcl11b is required for differentiation and survival of αβ T lymphocytes. *Nat Immunol* **4**: 533–539.

Walworth N, Davey S, Beach D. (1993). Fission yeast chk1 protein kinase links the rad checkpoint pathway to cdc2. *Nature* **363**: 368–371.

Zhao H, Watkins JL, Piwnica-Worms H. (2002). Disruption of the checkpoint kinase 1/cell division cycle 25A pathway abrogates ionizing radiation-induced S and G2 checkpoints. *Proc Natl Acad Sci USA* **99**: 14795–14800.

Zhou BB, Bartek J. (2004). Targeting the checkpoint kinases: chemosensitization versus chemoprotection. *Nat Rev Cancer* **4**: 216–225.

Zou L, Elledge SJ. (2003). Sensing DNA damage through ATRIP recognition of RPA-ssDNA complexes. *Science* **300**: 1542–1548.

Supplementary Information accompanies the paper on the Oncogene website (http://www.nature.com/onc).

Aqueous and ethanolic extract fractions from the Brazilian propolis suppress azoxymethane-induced aberrant crypt foci in rats

YUMIKO YASUI[1], SHINGO MIYAMOTO[2], MIHYE KIM[1], HIROYUKI KOHNO[1], SHIGEYUKI SUGIE[1] and TAKUJI TANAKA[1]

[1]Department of Oncologic Pathology, Kanazawa Medical University, 1-1 Daigaku, Uchinada, Ishikawa 920-0293; [2]Division of Food Science and Biotechnology, Graduate School of Agriculture, Kyoto University, Kyoto 606-8502, Japan

Received February 20, 2008; Accepted April 30, 2008

DOI: 10.3892/or_00000033

Abstract. We investigated the effects of the two fractions, aqueous (AEP) and ethanolic extracts of propolis (EEP) of the Brazilian propolis on azoxymethane (AOM)-induced aberrant crypt foci (ACF). Male Wistar Hannover (GALAS) rats were administered two weekly subcutaneous injections of AOM (20 mg/kg bw) and fed with diets mixed with AEP (100, 500 and 1,000 ppm) or EEP (500 and 1,000 ppm) for 4 weeks, starting one week before the first dosing of AOM. The modifying effects of the test extracts on ACF formation were assessed by counting the incidence and multiplicity of ACF at week 4. Proliferation cell nuclear antigen (PCNA)-labeling nuclei and apoptotic index were also immunohistochemically determined. Dietary supplementation with AEP and EEP significantly reduced the multiplicity of ACF with the effect of EEP being more potent than AEP. In the ACF and their surrounding non-lesional crypts, significantly lowered cell proliferation was observed in the rats, administered with AOM, and the extracts, while neither fraction affected the apoptotic index. Our findings suggest that AEP and EEP possess a chemopreventive ability in the early phase of colon carcinogenesis through the modulation of cell proliferation.

Correspondence to: Dr Yumiko Yasui, Department of Oncologic Pathology, Kanazawa Medical University, 1-1 Daigaku, Uchinada, Ishikawa 920-0293, Japan
E-mail: y-yasui@kanazawa-med.ac.jp

Abbreviations: AEP, aqueous extract of propolis; EEP, ethanolic extract of propolis; AOM, azoxymethane; ACF, aberrant crypt foci; PCNA, proliferation cell nuclear antigen; CRC, colorectal cancer; EtOH, ethanol; ssDNA, single-stranded DNA

Key words: propolis, aqueous extract, ethanolic extract, chemoprevention, aberrant crypt foci, rats

Introduction

The high incidence of colorectal cancer (CRC) is a major public health problem in the United States and other Western countries (1). In Japan, the prevalence of CRC and the percentage of occurrence of this cancer among cancer deaths are increasing (2). Although the etiology of CRC development is multifactorial and complex, a great deal of effort has been made in the identification of naturally occurring and related synthetic agents that prevent CRC development. Numerous naturally occurring compounds such as phenols, indoles, inositol-6-phosphate, aromatic isothiocyanates and dithiolethiones were shown to inhibit several types of cancer, including CRC, in preclinical studies using laboratory animal models (3,4).

Propolis is a natural product that is derived from plant resins collected by honeybees. Propolis, used in folk medicine for centuries contains a variety of compounds including polyphenolics, flavones, flavonones, phenolic acid and esters, and fatty acids (5). Capillary zone electrophoresis revealed that different flavonoids, such as chrysin, rutin, catechin, myricetin, luteolin and quercetin, two phenolic acids (cinnamic and caffeic acids), and a stilbene derivative, resveratrol, are found in propolis extracts (6). The composition of the propolis depends upon the vegetation of the area from where it was collected and on the bee species. Brazilian propolis specifically contains artepillin C, because the bees collect materials from the Brazilian plant, *Baccharis dracunculifolia*, which contains a large amount of antioxidative artepillin C (7,8). Propolis has a variety of biological activities. They include anticarcinogenic (9), antioxidative (10), anti-inflammatory (11) and antibiotic (12) activities. Propolis has attracted much attention in recent years as a potential substance used for medicine and cosmetics. Several studies have reported on the anticarcinogenic activity of propolis in the colon (13,14). The active compounds of propolis are considered to be artepillin C (15) and caffeic acid (14), which are present in the ethanolic extract of propolis. Therefore, biological activities of the ethanolic rather than aqueous extract from propolis are attractive. However, few studies dealing with biological

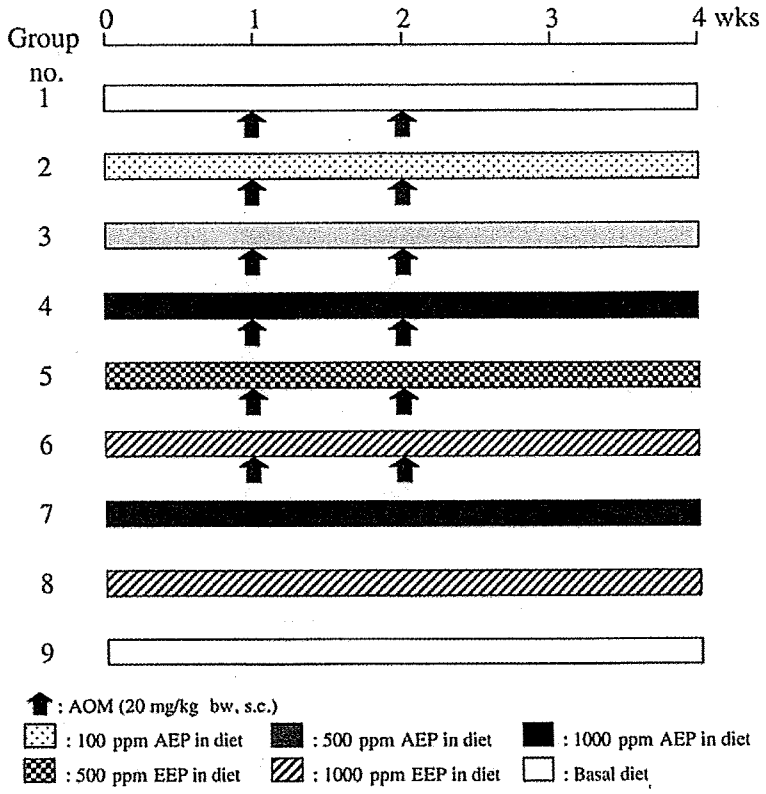

Figure 1. The experimental protocol.

activities, including the neuroprotective (16) and antimutagenic effects (17), of the aqueous extract of propolis exist.

In the present study, we determined whether the aqueous fraction from the Brazilian propolis extracts prevents the formation of aberrant crypt foci (ACF), which are a putative precursor lesion for CRC (18), induced by azoxymethane (AOM) in the rat colon. The effects were compared with those of the ethanolic extract.

Materials and methods

Preparation of fractions from Brazilian propolis extracts. Brazilian propolis was obtained from the Yamada Apiculture Center (Okayama, Japan). Brazilian propolis (100 g) was extracted with 60% ethanol (EtOH) at room temperature to yield the extract. The EtOH extract was filtrated, evaporated and lyophilized. H_2O was added to the extracts, and then filtrated. The filtrate was lyophilized to give an aqueous fraction (AEP, 14 g), and the residue was further extracted with EtOH to give an ethanolic fraction (EEP, 35 g). AEP and EEP were identified using a Delta 600E system (Nihon Waters, Tokyo, Japan) equipped with a Waters 2996 photodiode-array detection system. The used column was Cosmosil 5C18-AR-II (Φ4.6x250+Φ4.6x20 mm) (Nacalai Tesque Inc., Kyoto, Japan). The flow rate was 1 ml/min. We then identified the ingredients in the fractions by 1H NMR spectroscopy (ECA600 spectrometer, JEOL Ltd., Tokyo, Japan) and MS analysis (SX102A spectrometer, JEOL Ltd.). The analysis revealed that AEP contained the following acids: 13.5% 4,5-dicaffeoylquinic, 13.4% 3,5-dicaffeoylquinic, 4.9% *p*-coumaric, 1.7% chlorogenic, 1.3% 3,4-dicaffeoylquinic, 0.6% 4-caffeoylquinic, 0.2% 3-caffeoylquinic and 0.2% caffeic. The main ingredients of EEP were artepillin C (17.3%) and (E)-3-prenyl-4(2,3-dihydrocinnamoyloxy) cinnamic acid (11.8%). We were not able to determine chemistry of other components in EEP.

Animals, chemicals and diets. Male Wistar Hannover (GALAS) rats (19) aged 4 weeks purchased from CLEA Japan, Inc. (Tokyo, Japan) were used in the ACF assay. The animals were maintained in the Kanazawa Medical University Animal Facility according to the Institutional Animal Care Guidelines. The animals were housed in plastic cages (4 rats/cage) with free access to drinking water and a basal diet, CRF-1 (Oriental Yeast Co., Ltd., Tokyo, Japan) under controlled conditions of humidity (50±10%), lighting (12-h light/dark cycle) and temperature (23±2°C). The animals were quarantined for 7 days after arrival and randomized by body weight into experimental and control groups (Fig. 1). Beginning at 5 weeks of age, they were fed with experimental diets for 4 weeks. The rats in groups 1 (11 rats) and 9 (4 rats) were fed the basal diet alone. Groups 2-4 (8 rats each) were fed the diets containing 100, 500 and 1,000 ppm of AEP, respectively. Groups 5 and 6 (8 rats each) were given the diets containing 500 and 1,000 ppm of EEP, respectively. Groups 7 and 8 (4 rats each) were fed the diets containing 1000 ppm of AEP and EEP alone, respectively. All rats were freely available for the experimental and basal diets and tap water, and weighed weekly. At 6 weeks of age, the animals in groups 1-6 were given two subcutaneous injections of

Table I. Body, liver and relative liver weights.

Group no.	Treatment	No. of rats examined	Body weight (g)	Liver weight (g)	Relative liver weight (g/100 g body weight)
1	AOM	11	266±22[a]	12.3±2.8	4.59±0.70
2	AOM+AEP (100 ppm)	8	263±11	13.6±1.3	5.17±0.39
3	AOM+AEP (500 ppm)	8	255±15	12.1±1.1	4.71±0.25
4	AOM+AEP (1000 ppm)	8	255±16	12.9±1.6	5.03±0.39
5	AOM+EEP (500 ppm)	8	260±15	13.1±1.6	5.03±0.39
6	AOM+EEP (1000 ppm)	8	253±14	12.0±0.9	4.72±0.24
7	AEP (1000 ppm)	4	253±13	11.8±1.3	4.62±0.31
8	EEP (1000 ppm)	4	252±3	12.9±0.6	5.10±0.26
9	None	4	244±15	10.7±1.6	4.36±0.35

[a]Means ± SD.

AOM (20 mg/kg body weight, Sigma-Aldrich Chemical Co., St. Louis, MO, USA) to induce ACF. The animals were sacrificed 2 weeks after the last administration of AOM, and complete necropsies were performed. Eight rat colons from group 1 and 5 rat colons each from groups 2-9 were subjected to determine the presence of ACF.

Determination of ACF. The number of ACF per colon was determined according to the method described in our previous report (20). At autopsy, the colons were flushed with saline, excised, cut open longitudinally along the main axis and then washed with saline. They were cut, and fixed in 10% buffered formalin for at least 24 h. Fixed colons were dipped in a 0.5% solution of methylene blue in distilled water for 30 sec, briefly washed with the distilled water, and placed on microscope slides with the mucosal surface up. Using a light microscope (Olympus BX41, Olympus Optical Co., Ltd., Tokyo, Japan) at a magnification of x40, ACF were counted. After counting ACF, the colonic tissues were routinely processed for tissue preparation for histopathology and immunohistochemistry.

Immunohistochemistry. Immunohistochemistry for the proliferating cell nuclear antigen (PCNA) and apoptotic nuclei was performed on 4-μm thick paraffin-embedded sections from the rat colons in each group by the labeled streptavidin biotin method using an LSAB kit (Dako Japan, Kyoto, Japan) with microwave accentuation. The paraffin-embedded sections were heated for 30 min at 65˚C, deparaffinized in xylene, and rehydrated through graded ethanol at room temperature. Tris HCl buffer (0.05 M, pH 7.6) was used to prepare solutions and for washes between various steps. Incubations were performed in a humidified chamber. To determine the PCNA-incorporated nuclei, PCNA immunohistochemistry was performed according to the method described by Watanabe *et al* (21). The apoptotic index was also evaluated by immunohistochemistry for single-stranded DNA (ssDNA) (21). Sections were treated for 40 min at room temperature with 2% BSA and incubated overnight at 4˚C with primary antibodies. These antibodies included anti-PCNA mouse monoclonal antibody (diluted 1:50, PC10, Dako Japan), and anti-ssDNA rabbit polyclonal antibody (diluted 1:300, Dako Japan). Horseradish peroxidase activity was visualized by treatment with H_2O_2 and 3,3'-diaminobenzidine for 5 min. At the final step, the sections were weakly counterstained with Mayer's hematoxylin (Merck Ltd., Tokyo, Japan). For each case, negative controls were performed on serial sections. On the control sections, incubation with the primary antibodies was omitted. The intensity and localization of immunoreactivity against the two primary antibodies used were examined on all sections using a microscope, Olympus BX41 (Olympus Optical Co., Ltd.). The PCNA and apoptotic indices were determined by counting the number of positive nuclei at least 100 cells each in the lesional or normal-appearing crypts, and were expressed as percentages.

Statistical analysis. All measurements were statistically analyzed using one-way ANOVA followed by Tukey-Kramer post-hoc test for multiple comparison test (GraphPad Instat version 3.05, GraphPad Softwear, San Diego, CA, USA). Differences were considered to be statistically significant at $P<0.05$.

Results

Table I shows the body, liver and relative liver weights of the rats in all groups. The animals remained healthy throughout the experimental period. The mean body, liver and relative liver weights did not significantly differ among the groups.

Frequency of ACF. Table II summarizes the data of the colonic ACF analysis. The rats belonging to groups 1-6 that received AOM, developed ACF (Fig. 2a and b). ACF were not observed in rats in groups 7-9 that were not administered AOM. The mean number of ACF/colon of group 1 was 38.8±19.9. The dietary administration of AEP and EEP at all the dose levels caused significant inhibition of ACF formation: 100 ppm AEP, 14.2±5.2 (63% reduction, $P<0.01$); 500 ppm AEP, 8.8±8.7 (77% reduction, $P<0.01$); 1,000 ppm AEP, 10.6±6.9 (73% reduction, $P<0.01$); 500 ppm EEP, 7.2±5.4

Table II. Effects of AEP and EEP of the extracts from propolis on AOM which induces ACF in rat colons.

Group no.	Treatment	No. of rats examined	No. of ACF/ colon	No. of ACF consisted of >4 crypts/colon	Total no. of aberrant crypts (ACs)/colon	ACs/focus
1	AOM	8	38.8±19.9[a]	9.5±7.8	109.5±78.6	2.65±0.90
2	AOM+AEP (100 ppm)	5	14.2±5.2[b]	0.2±0.4[b]	18.0±8.2[b]	1.25±0.21[c]
3	AOM+AEP (500 ppm)	5	8.8±8.7[b]	0[b]	11.2±11.4[b]	1.25±0.28[c]
4	AOM+AEP (1000 ppm)	5	10.6±6.9[b]	0.2±0.4[b]	16.0±11.2[b]	2.51±0.13
5	AOM+EEP (500 ppm)	5	7.2±5.4[c]	0[b]	9.6±7.8[b]	1.31±0.27[c]
6	AOM+EEP (1000 ppm)	5	6.4±4.3[c]	0[b]	7.6±5.6[b]	1.41±0.16[c]

[a]Means ± SD. [b,c]Significantly different from group 1 by Tukey-Kramer multiple comparison test ([b]P<0.01 and [c]P<0.001).

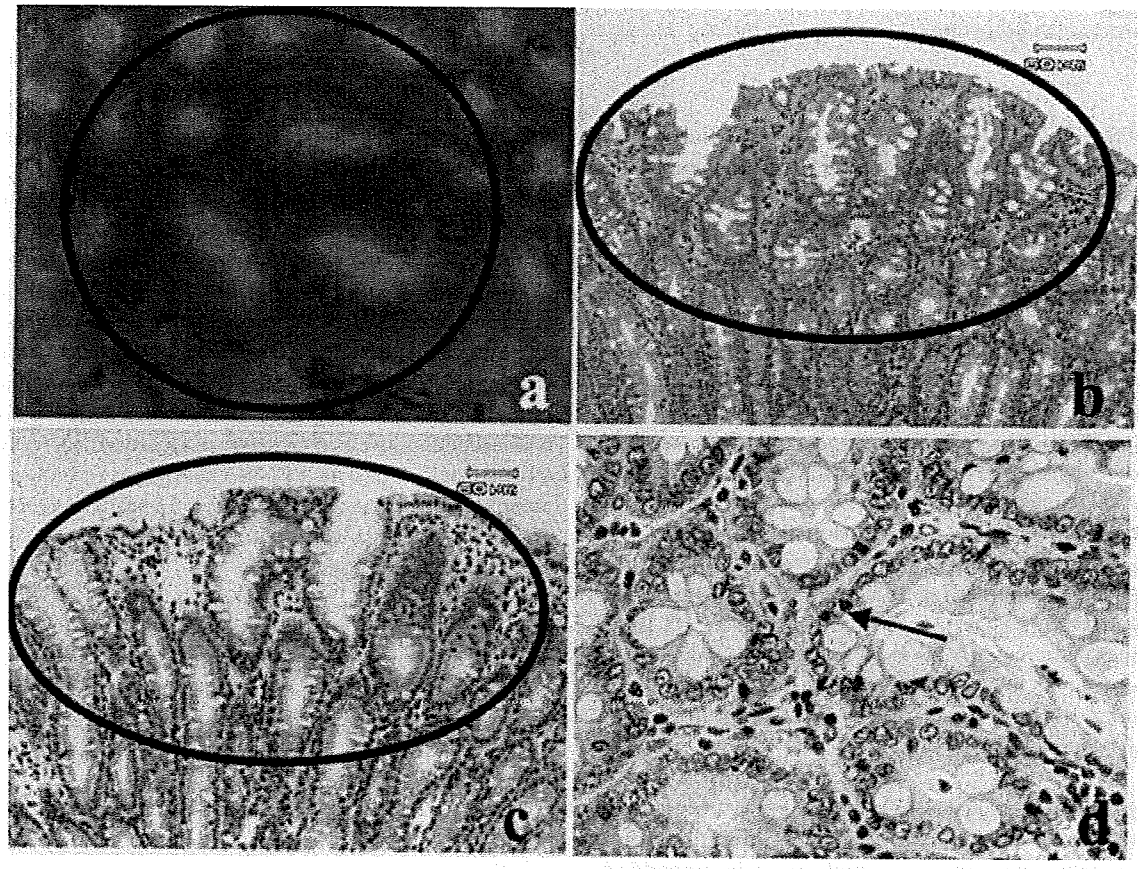

Figure 2. Histopathology and immunohistochemistry of PCNA and ssDNA. (a) ACF (circled) stained by methylene blue consisting of three aberrant crypts (group 1); (b) ACF (circled) stained with hematoxylin and eosin consisting of five aberrant crypts (group 1); (c) PCNA immunohistochemistry of ACF consisting of five aberrant crypts and (d) ssDNA immunohistochemistry of non-lesional crypts. The arrow indicates an ssDNA-positive nucleus (apoptotic nucleus). Original magnification: (a) x20; (b) x50; (c) x50 and (d) x200.

(81% reduction, P<0.001) and 1,000 ppm EEP, 6.4±4.3 (84% reduction, P<0.001). There were significant decreases in the total number of aberrant crypts (ACs) per colon (P<0.01) in groups 2-6, and the number of ACs per focus (P<0.01) in these groups except for group 4. The numbers of ACF consisting of >4 crypts in groups 2-6 were significantly smaller than that of group 1 (P<0.01).

PCNA-labeling index. The PCNA-labeling index in the ACF (Fig. 2c) and normal-appearing crypts are presented in Table III. As for the mean PCNA-labeling index of ACF, the values of groups 3 (18.4±3.0, P<0.001) and 4 (14.0±1.6, P<0.001), which were treated with 500 and 1,000 ppm of AEP, respectively, were significantly decreased when compared with group 1 (26.6±3.6), although group 2 (21.4±2.1), which was treated with 100 ppm AEP, was insignificantly reduced. The indices of groups 5 (13.4±2.1, P<0.001) and 6 (12.2±4.2, P<0.001), which were treated with 500 and 1,000 ppm of EEP alone, respectively, were significantly reduced when compared with group 1. The mean PCNA-labeling indices in

Table III. PCNA-labeling and apoptotic index in ACF and colonic crypts of rats treated with AOM and/or AEP and EEP of the extracts from propolis.

Group no.	Treatment	PCNA-labeling index (%)		Apoptosis index (%)	
		ACF	Normal-appearing crypt	ACF	Normal-appearing crypt
1	AOM	26.6±3.6[a] (8)	19.1±2.0 (8)	4.1±0.8 (8)	0.47±0.11 (8)
2	AOM+AEP (100 ppm)	21.4±2.1 (5)	16.0±3.2 (5)	4.8±2.4 (5)	0.49±0.12 (5)
3	AOM+AEP (500 ppm)	18.4±3.0[b] (5)	12.4±2.7[b] (5)	6.4±2.7 (5)	0.46±0.19 (5)
4	AOM+AEP (1000 ppm)	14.0±1.6[b,c] (5)	12.8±1.9[b] (5)	5.8±1.5 (5)	0.48±0.13 (5)
5	AOM+EEP (500 ppm)	13.4±2.1[b] (5)	11.2±2.3[b] (5)	6.2±1.8 (5)	0.49±0.10 (5)
6	AOM+EEP (1000 ppm)	12.2±4.2[b] (5)	10.4±2.2[b] (5)	6.6±1.5 (5)	0.48±0.15 (5)
7	AEP (1000 ppm)	-	9.4±1.1[b] (5)	-	0.40±0.18 (5)
8	EEP (1000 ppm)	-	9.4±1.8[b] (5)	-	0.38±0.11 (5)
9	None	-	9.8±1.5[b] (5)	-	0.37±0.14 (5)

The numbers in parentheses indicate the number of rats examined. [a]Means ± SD. [b]Significantly different from group 1 by Tukey-Kramer multiple comparison test ([b]P<0.001). [c,d]Significantly different from group 2 by Tukey-Kramer's multiple comparison test ([c]P<0.01).

normal-appearing crypts of groups 1-6 were higher than those of groups 7-9. Dietary feeding with AEP and EEP at all doses, except for group 2, significantly reduced the mean PCNA-labeling indices when compared with group 1 (P<0.001).

Apoptotic index. The mean apoptotic indices in ACF (Fig. 2d) and normal-appearing crypts are presented in Table III. The mean apoptotic indices increased by treatment with AEP or EEP, but did not significantly differ among the groups.

Discussion

In the present study, we demonstrated that aqueous (AEP) and ethanolic fractions (EEP) extracted from Brazilian propolis exerted an inhibitory effect on ACF formation. Feeding with AEP and EEP decreased the number of large ACF which reflects colon cancer development (22).

In this study, dietary AEP significantly suppressed the ACF formation induced by AOM, but the effect was not dose-dependent. Our findings, however, suggest that 500 ppm of AEP is the optimum dose to exert its ACF-inhibiting effect. Noteworthy findings in this study are that feeding with AEP as well as EEP was able to lower the cell proliferation activity in the ACF and their surrounding normal-appearing crypts, but did not affect apoptosis. de Lima *et al* reported that the aqueous extract of Brazilian propolis can modulate the DNA damage induced by DMH (23). When the effects of AEP were evaluated on the formation of DMH-induced ACF and DNA damage in the colon of male Wistar rats by the ACF and Comet assays, respectively, AEP showed no statistically significant reduction of ACF either simultaneously with or after DMH treatment. However, AEP administered simultaneously with DMH, reduced DNA damage induction in the mid and distal colon. The difference of the effects of AEP of ACF formation between their study and our study may be due to the difference of strain of rats used. A water extract of Brazilian green propolis has recently been reported to inhibit doxorubicin-induced somatic mutation (24). Our study demonstrated that chrysin, present in an ethanolic extract of propolis, has a chemopreventive activity in ACF occurrence in rats initiated with AOM (25). Taken together, propolis extracts, either aqueous or ethanolic, affect proliferation and result in the inhibition of ACF development.

Several studies have indicated anticarcinogenic activity of propolis in the colon. Dietary propolis significantly reduced the number of colonic ACF induced by 1,2-dimethylhydrazine (DMH) in rats (13). Caffeic acid esters, which are present in the ethanolic extract of propolis, suppressed ACF induced by AOM and inhibited the activities of ornithine decarboxylase,

tyrosine protein kinase, and lipoxygenase in the colon and liver (14). Among the constituents of propolis, artepillin C is considered to be responsible for the anticancer property of propolis. Artepillin C induces cell-cycle arrest via stimulation of Cip1/p21 expression in the human colon cancer cells, Caco-2 (26). Dietary artepillin C also suppresses ACF development in conjunction with the induction of phase II enzymes in liver in mice initiated with AOM (15). Although several reports exist demonstrating the cancer chemopreventive effects of other ingredients in propolis, such as caffeic acid ester (14,27), cinnamic acid (28) and galagin (29), few experiments investigating the chemopreventive ability of propolis extracts or fractions exist.

In the AEP used in this study, the main ingredients are dicaffeoylquinic acid isomers, *p*-coumaric acid and chlorogenic acid as reported previously (30). Notably, 3,4-, 3,5- and 4,5-di-*O*-dicaffeoylquinic acid isolated from the sweet potato (*Ipomoea batatas L.*) possesses anti-mutagenic activity in the reverse mutation of *Salmonella typhimurium* TA 98 induced by the 3-amino-1,4-dimethyl-5H-pyrido(4,3-*b*) indole (17). A water extract of Brazilian green propolis and its main ingredients of caffeoylquinic acid derivatives (3,4-di-*O*-caffeoylquinic, 3,5-di-*O*-caffeoyl-quinic and chlorogenic acids), have antioxidant effects (16). Although dicaffeoylquinic acid possesses antioxidant activity (31,32), its chemopreventive effects of carcinogenesis have yet to be reported. *p*-Coumaric acid with antioxidative ability (33) inhibits cell proliferation by affecting cell cycle phases in the human colonic cell line Caco-2 (34), and significantly decreased the mutagenicity of Glu-P-2 (35). Dietary chlorogenic acid, a prominent antioxidant (36), prevents the development of the AOM-induced ACF in rat colon (37) and inhibits DNA methylation in human breast cancer cells (38). Therefore, these biological activities of the main constituent of AEP may contribute to the reduction of ACF formation in this study.

In conclusion, our results suggest that AEP (mainly containing dicaffeoylquinic acid isomers) as well as EEP isolated from the Brazilian propolis exert inhibitory activities against AOM-induced colonic ACF. Their suppressing effects may be due to the suppression of cell proliferation without affecting apoptosis.

Acknowledgements

This work was supported in part by a Grant-in-Aid for Cancer Research, for the Third-Term Comprehensive 10-Year Strategy for Cancer Control from the Ministry of Health, Labour and Welfare of Japan; a Grant-in-Aid (no. 18880030 to Y.Y., 18592076 to T.T. and 17015016 to T.T.) for Scientific Research from the Ministry of Education, Culture, Sports, Science and Technology of Japan; and grants (S2006-9 to Y.Y. and H2007-12 to T.T.) for the Project Research from the High-Technology Center of Kanazawa Medical University. The authors wish to thank Prof. Toshifumi Hirata, Ph.D. (Department of Mathematical and Life Sciences, Hiroshima University, Japan) for his analysis of extracts of Brazilian propolis.

References

1. Boring CC, Squires TS and Tong T: Cancer statistics. CA Cancer J Clin 43: 7-26, 1993.
2. Minami Y, Nishino Y, Tsubono Y, Tsuji I and Hisamichi S: Increase of colon and rectal cancer incidence rates in Japan: trends in incidence rates in Miyagi Prefecture, 1959-1997. J Epidemiol 16: 240-248, 2006.
3. Bertram JS, Kolonel LN and Meyskens FL: Rationale and strategies for chemoprevention of cancer in humans. Cancer Res 47: 3012-3031, 1987.
4. Boone CW, Kelloff GJ and Malone WE: Identification of candidate cancer chemopreventive agents and their evaluation in animal models and human clinical trials: a review. Cancer Res 50: 2-9, 1990.
5. Ivanov T: Composition and physico-chemical properties of propolis. Zhivotnovudni Nauki 17: 96-103, 1980.
6. Volpi N: Separation of flavonoids and phenolic acids from propolis by capillary zone electrophoresis. Electrophoresis 25: 1872-1878, 2004.
7. Kimoto T, Koya S, Hino K, Yamamoto Y, Nomura Y, Micallef MJ, Hanaya T, Arai S, Ikeda M and Kurimoto M: Renal carcinogenesis induced by ferric nitrilotriacetate in mice, and protection from it by Brazilian propolis and artepillin C. Pathol Int 50: 679-689, 2000.
8. Matsuno T, Jung SK, Matsumoto Y, Saito M and Morikawa J: Preferential cytotoxicity to tumor cells of 3,5-diprenyl-4-hydroxycinnamic acid (artepillin C) isolated from propolis. Anticancer Res 17: 3565-3568, 1997.
9. Grunberger D, Banerjee R, Eisinger K, Oltz EM, Efros L, Caldwell M, Estevez V and Nakanishi K: Preferential cytotoxicity on tumor cells by caffeic acid phenethyl ester isolated from propolis. Experientia 44: 230-232, 1988.
10. Pascual C, Gonzalez R and Torricella RG: Scavenging action of propolis extract against oxygen radicals. J Ethnopharmacol 41: 9-13, 1994.
11. Khayyal MT, el-Ghazaly MA and el-Khatib AS: Mechanisms involved in the antiinflammatory effect of propolis extract. Drugs Exp Clin Res 19: 197-203, 1993.
12. Kujumgiev A, Bankova V, Ignatova A and Popov S: Antibacterial activity of propolis, some of its components and their analogs. Pharmazie 48: 785-786, 1993.
13. Bazo AP, Rodrigues MA, Sforcin JM, de Camargo JL, Ribeiro LR and Salvadori DM: Protective action of propolis on the rat colon carcinogenesis. Teratog Carcinog Mutagen 22: 183-194, 2002.
14. Rao CV, Desai D, Simi B, Kulkarni N, Amin S and Reddy BS: Inhibitory effect of caffeic acid esters on azoxymethane-induced biochemical changes and aberrant crypt foci formation in rat colon. Cancer Res 53: 4182-4188, 1993.
15. Shimizu K, Das SK, Baba M, Matsuura Y and Kanazawa K: Dietary artepillin C suppresses the formation of aberrant crypt foci induced by azoxymethane in mouse colon. Cancer Lett 240: 135-142, 2006.
16. Nakajima Y, Shimazawa M, Mishima S and Hara H: Water extract of propolis and its main constituents, caffeoylquinic acid derivatives, exert neuroprotective effects via antioxidant actions. Life Sci 80: 370-377, 2007.
17. Yoshimoto M, Yahara S, Okuno S, Islam MS, Ishiguro K and Yamakawa O: Antimutagenicity of mono-, di-, and tricaffeoylquinic acid derivatives isolated from sweetpotato (*Ipomoea batatas L.*) leaf. Biosci Biotechnol Biochem 66: 2336-2341, 2002.
18. Bird RP: Role of aberrant crypt foci in understanding the pathogenesis of colon cancer. Cancer Lett 93: 55-71, 1995.
19. Aoyama H, Kikuta M, Shirasaka N, Hojo H, Takahashi KL, Shimizu N, Harigae M, Taguchi F and Teramoto S: Historical control data on reproductive abilities and incidences of spontaneous fetal malformations in Wistar Hannover GALAS rats. Congenit Anom 42: 194-201, 2002.
20. Tanaka T, Kawabata K, Kakumoto M, Makita H, Hara A, Mori H, Satoh K, Hara A, Murakami A, Kuki W, Takahashi Y, Yonei H, Koshimizu K and Ohigashi H: Citrus auraptene inhibits chemically induced colonic aberrant crypt foci in male F344 rats. Carcinogenesis 18: 2155-2161, 1997.
21. Watanabe I, Toyoda M, Okuda J, Tenjo T, Tanaka K, Yamamoto T, Kawasaki H, Sugiyama T, Kawarada Y and Tanigawa N: Detection of apoptotic cells in human colorectal cancer by two different in situ methods: antibody against single-stranded DNA and terminal deoxynucleotidyl transferase-mediated dUTP-biotin nick end-labeling (TUNEL) methods. Jpn J Cancer Res 90: 188-193, 1999.

22. Pretlow TP, O'Riordan MA, Somich GA, Amini SB and Pretlow TG: Aberrant crypts correlate with tumor incidence in F344 rats treated with azoxymethane and phytate. Carcinogenesis 13: 1509-1512, 1992.
23. de Lima RO, Bazo AP, Said RA, Sforcin JM, Bankova V, Darros BR and Salvadori DM: Modifying effect of propolis on dimethylhydrazine-induced DNA damage but not colonic aberrant crypt foci in rats. Environ Mol Mutagen 45: 8-16, 2005.
24. Valadares BL, Graf U and Spano MA: Inhibitory effects of water extract of propolis on doxorubicin-induced somatic mutation and recombination in *Drosophila melanogaster*. Food Chem Toxicol 46: 1103-1110, 2008.
25. Miyamoto S, Kohno H, Suzuki R, Sugie S, Murakami A, Ohigashi H and Tanaka T: Preventive effects of chrysin on the development of azoxymethane-induced colonic aberrant crypt foci in rats. Oncol Rep 15: 1169-1173, 2006.
26. Shimizu K, Das SK, Hashimoto T, Sowa Y, Yoshida T, Sakai T, Matsuura Y and Kanazawa K: Artepillin C in Brazilian propolis induces G(0)/G(1) arrest via stimulation of Cip1/p21 expression in human colon cancer cells. Mol Carcinog 44: 293-299, 2005.
27. Xiang D, Wang D, He Y, Xie J, Zhong Z, Li Z and Xie J: Caffeic acid phenethyl ester induces growth arrest and apoptosis of colon cancer cells via the beta-catenin/T-cell factor signaling. Anticancer Drugs 17: 753-762, 2006.
28. Akao Y, Maruyama H, Matsumoto K, Ohguchi K, Nishizawa K, Sakamoto T, Araki Y, Mishima S and Nozawa Y: Cell growth inhibitory effect of cinnamic acid derivatives from propolis on human tumor cell lines. Biol Pharm Bull 26: 1057-1059, 2003.
29. Heo MY, Sohn SJ and Au WW: Anti-genotoxicity of galangin as a cancer chemopreventive agent candidate. Mutat Res 488: 135-150, 2001.
30. Sawaya AC, Tomazela DM, Cunha IB, Bankova VS, Marcucci MC, Custodio AR and Eberlin MN: Electrospray ionization mass spectrometry fingerprinting of propolis. Analyst 129: 739-744, 2004.
31. Kim HJ and Lee YS: Identification of new dicaffeoylquinic acids from *Chrysanthemum morifolium* and their antioxidant activities. Planta Med 71: 871-876, 2005.
32. Hung TM, Na M, Thuong PT, Su ND, Sok D, Song KS, Seong YH and Bae K: Antioxidant activity of caffeoylquinic acid derivatives from the roots of Dipsacus asper Wall. J Ethnopharmacol 108: 188-192, 2006.
33. Tsai PJ and She CH: Significance of phenol-protein interactions in modifying the antioxidant capacity of peas. J Agric Food Chem 54: 8491-8494, 2006.
34. Janicke B, Onning G and Oredsson SM: Differential effects of ferulic acid and p-coumaric acid on S phase distribution and length of S phase in the human colonic cell line Caco-2. J Agric Food Chem 53: 6658-6665, 2005.
35. Yamada J and Tomita Y: Antimutagenic activity of caffeic acid and related compounds. Biosci Biotechnol Biochem 60: 328-329, 1996.
36. Jung HA, Park JC, Chung HY, Kim J and Choi JS: Antioxidant flavonoids and chlorogenic acid from the leaves of *Eriobotrya japonica*. Arch Pharm Res 22: 213-218, 1999.
37. Morishita Y, Yoshimi N, Kawabata K, Matsunaga K, Sugie S, Tanaka T and Mori H: Regressive effects of various chemopreventive agents on azoxymethane-induced aberrant crypt foci in the rat colon. Jpn J Cancer Res 88: 815-820, 1997.
38. Lee WJ and Zhu BT: Inhibition of DNA methylation by caffeic acid and chlorogenic acid, two common catechol-containing coffee polyphenols. Carcinogenesis 27: 269-277, 2006.

Int. J. Radiation Oncology Biol. Phys., Vol. 77, No. 1, pp. 235–243, 2010

0360-3016/10/$–see front matter

ELSEVIER

doi:10.1016/j.ijrobp.2009.11.005

BIOLOGY CONTRIBUTION

CLONALLY EXPANDING THYMOCYTES HAVING LINEAGE CAPABILITY IN GAMMA-RAY–INDUCED MOUSE ATROPHIC THYMUS

TAKASHI YAMAMOTO, M.D.,*† SHIN-ICHI MORITA, M.D.,*† RIEKA GO, D.D.S.,* MIKI OBATA, B.SCI.,* YOSHINORI KATSURAGI, PH.D.,* YUKARI FUJITA, M.SCI.,* YOSHITAKA MAEDA, B.SCI.,‡ MINESUKE YOKOYAMA, PH.D.,‡ YUTAKA AOYAGI, M.D., PH.D.,† HITOSHI ICHIKAWA, PH.D.,§ YUKIO MISHIMA, PH.D.,* AND RYO KOMINAMI, M.D., PH.D.*

*Department of Molecular Genetics and †3rd Internal Medicine, Niigata University Graduate School of Medical and Dental Sciences, Niigata, Japan; ‡Center for Bioresource-Based Researches, Brain Research Institute, Niigata, Japan; and §Genetics Division, National Cancer Center Research Institute, Tokyo, Japan

Purpose: To characterize, in the setting of γ-ray–induced atrophic thymus, probable prelymphoma cells showing clonal growth and changes in signaling, including DNA damage checkpoint.
Methods and Materials: A total of 111 and 45 mouse atrophic thymuses at 40 and 80 days, respectively, after γ-irradiation were analyzed with polymerase chain reaction for D-J rearrangements at the *TCRβ* locus, flow cytometry for cell cycle, and Western blotting for the activation of DNA damage checkpoints.
Results: Limited D-J rearrangement patterns distinct from normal thymus were detected at high frequencies (43 of 111 for 40-day thymus and 21 of 45 for 80-day thymus). Those clonally expanded thymocytes mostly consisted of $CD4^+CD8^+$ double-positive cells, indicating the retention of lineage capability. They exhibited pausing at a late G1 phase of cell cycle progression but did not show the activation of DNA damage checkpoints such as γH2AX, Chk1/2, or p53. Of interest is that 17 of the 52 thymuses showing normal D-J rearrangement patterns at 40 days after irradiation showed allelic loss at the *Bcl11b* tumor suppressor locus, also indicating clonal expansion.
Conclusion: The thymocytes of clonal growth detected resemble human chronic myeloid leukemia in possessing self-renewal and lineage capability, and therefore they can be a candidate of the lymphoma-initiating cells. © 2010 Elsevier Inc.

Gamma-ray–induced mouse thymic lymphoma, Prelymphoma, DNA damage response, Bcl11b, Cancer stem cells.

INTRODUCTION

Premalignant conditions are recognizable lesions that are strongly associated with the development of malignant neoplasia. One such lesion must exist in γ-ray–induced mouse atrophic thymus because mice that received thymocytes from the atrophic thymus developed thymic lymphomas at a high frequency (1, 2). Immature thymocytes in the thymus proliferate and undergo β-selection at $CD4^-$ and $CD8^-$ double-negative stage and differentiate into double-positive (DP) cells, which further differentiate into $CD4^+$ or $CD8^+$ single-positive cells (3, 4). The thymus controls the cellular fate of thymocytes, including the elimination of unfavorable cells that are generated during developmental and pathologic processes (5).

Chronic myeloid leukemia (CML) may have a characteristic of the premalignant condition because CML cells differentiate to mature, nontumorigenic blood cells though possessing intrinsic self-renewal capability (6, 7). The transition from the CML chronic phase to the aggressive blast crisis phase requires the arrest of differentiation. Because CML arises from hematopoietic stem cell–like progenitors, it is thought to conform well to the cancer stem cell model (8). As described above, because of the tumorigenic capability of thymocytes in the atrophic thymus, thymocytes might contain cancer stem cells or lymphoma-initiating cells. The importance of leukemia-initiating cells is pointed out in relapsed acute lymphoblastic leukemia in humans, in that the cells responsible for relapse are ancestral to the primary leukemia cells (9).

Normal cells can perceive and arrest aberrant cycles of cell division that are triggered by cancer-promoting stimuli. A hallmark of precancerous cells in major human cancer types is aberrant stimulation of cell proliferation that results in

Reprint requests: Ryo Kominami, M.D., Department of Molecular Genetics, Niigata University Graduate School of Medical and Dental Sciences, Asahimachi 1-757, Chuo-ku, Niigata 951-8510, Japan. Tel: (+81) 25-227-2077; Fax: (+81) 25-227-0757; E-mail: rykomina@med.niigata-u.ac.jp

T.Y. and S.M. contributed equally to this work.

This work was supported by grants-in-aid for Cancer Research from the Ministries of Education, Science, Art and Sports, and Health and Welfare of Japan.

Conflict of interest: none.

Received Aug 20, 2009, and in revised form Nov 5, 2009. Accepted for publication Nov 7, 2009.

DNA replication stress and the subsequent activation of DNA damage checkpoint (10, 11). The checkpoint functions as an inducible barrier against genomic instability and tumor development (12, 13). The probable prelymphoma cells may exhibit the activation of DNA damage checkpoint, or they may show difference in oncogenic signals because lymphomas/leukemias are distinct in origin from carcinomas. Indeed, some disagreement has been reported in the study of T cell lymphomas developed in *PTEN*-deficient mice (14). In this study, we have characterized the probable prelymphoma cells showing clonal growth and changes in signaling, including DNA damage checkpoint.

METHODS AND MATERIALS

Mice and induction of atrophic thymus and lymphoma development

BALB/cAJcl mice (purchased from CLEA Japan, Tokyo, Japan) were mated with MSM mice (provided from Dr. Shiroishi, National Institute of Genetics at Mishima), and their male and female progeny were subjected to whole-body γ-irradiation of 2.5 Gy (^{137}Cs) four times at a weekly interval, starting at the age of 4 weeks. Thymus was isolated at 40 days and 80 days after the start of irradiation. Isolation of thymic lymphomas and bone marrow cell transfer were carried out as described previously (15, 16). Mice used in this study were maintained under specific pathogen-free conditions in the animal colony of Niigata University. All animal experiments comply with the guidelines of the animal ethics committee for animal experimentation of the University.

Flow cytometry

Flow cytometric analysis and 5-bromo-2-deoxyuridine (BrdU) incorporation experiments were performed as previously described (17). The monoclonal antibodies used were anti-CD4-FITC or -APC (RM4-5), anti-CD8-APC (53-6.7), purchased from eBioscience (San Diego, CA). Anti-Nrp-1 (sc-5541; Santa Cruz Biotechnology, Santa Cruz, CA) was detected with anti-rabbit IgG-Alexa Fluor 488 (A11008; Molecular Probes, Invitrogen, Carlsbad, CA.). Dead cells and debris were excluded from the analysis by appropriate gating of forward scatter (FSC) and side scatter (SSC). Cells were analyzed by a FACScan (Becton-Dickinson, Franklin Lakes, NJ) flow cytometer, and data were analyzed using Flow-Jo software (Tree-Star, Ashland, OR).

DNA isolation and PCR analysis

Deoxyribonucleic acid was isolated from brain, thymocytes, and thymic lymphomas using the DNeasy Tissue Kit (Qiagen, Valencia, CA). To determine D-J rearrangement patterns in the *TCRβ* locus, polymerase chain reaction (PCR) was performed as described previously (16). For allelic loss analysis at *Bcl11b*, *D12Mit53* and *D12Mit279* markers were used for PCR as described previously (15). The PCR products were analyzed by 8% polyacrylamide gel electrophoresis, and band intensities were quantitated with a Molecular Imager FX (Bio-Rad Laboratories, Hercules, CA) after ethidium bromide staining to determine the allele ratio of BALB/c and MSM alleles.

Antibodies for Western blotting

Sample preparation and Western blotting were performed as described previously (18). Antibodies used are listed below. Anti-H2AX (ab11175) and anti-Chk2 (pT68) (ab38461) were purchased from Abcam (Cambridge, MA). Anti-p27 Kip1 (#2552), anti-Chk2 (#2662), anti-p53 (pSer15) (#9284), anti-Akt (#9272), and anti-Akt (pSer473) (#4058) were purchased from Cell Signaling Technology (Danvers, MA). Anti-cMyc (sc-42), anti–proliferating cell nuclear antigen (PCNA) (sc-7907), anti-actin (sc-1615), anti-p53 (sc-1312), anti-Chk1 (sc7898), and horseradish peroxidase (HRP)-anti-goat IgG (sc-2020) were purchased from Santa Cruz Biotechnology. Anti-cyclin D1 (K0062-3) was purchased from MBL (Nagoya, Japan). Anti-Chk1(pS317) (AF473) was purchased from R&D Systems (Minneapolis, MN). Horseradish peroxidase-anti-rabbit IgG (NA934 V) and HRP-anti-mouse IgG (NA931VS) were purchased from Amersham (Piscataway, NJ). Anti-γH2AX (Ser139) (#07-164) was purchased from Upstate (Temecula, CA).

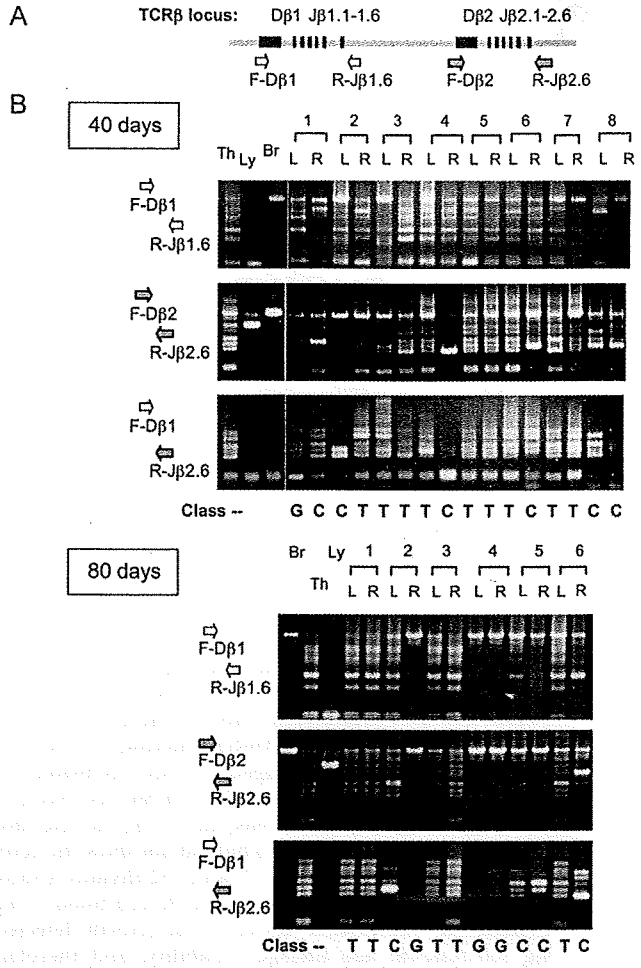

Fig. 1. Clonal growth of thymocytes in atrophic thymuses at 40 days and 80 days after γ-irradiation. (A) Diagram showing part of the *TCRβ* locus and the relative location of polymerase chain reaction (PCR) primers used. (B) Gel electrophoresis of PCR products with three different sets of primers: F-Dβ1 and R-Jβ1.6 (top), F-Dβ2 and to-Jβ2.6 (middle), and F-Dβ1 and R-Jβ2.6 (bottom). Th = thymus; Ly = lymphomas; Br = barain DNA; L and R = left and right thymic lobe; T = T type thymus; C = C type thymus; G = G type thymus.

RESULTS

Clonal expansion of thymocytes in γ-ray–induced atrophic thymus

Clonality of thymocytes was examined in left and right lobes separately of atrophic thymuses at 40 and 80 days after

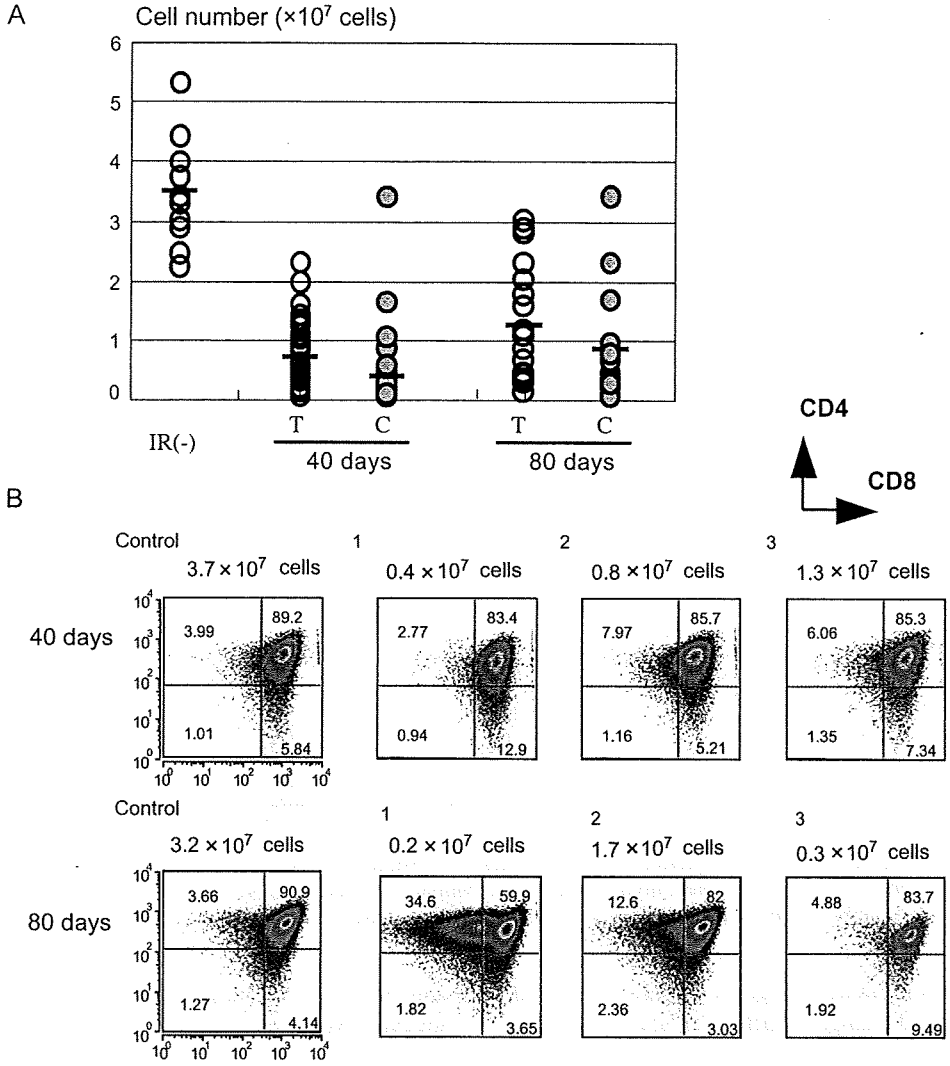

Fig. 2. Reduced cellularity and minimal changes of thymocyte differentiation in atrophic thymuses. (A) Cell numbers of thymocytes in unirradiated thymus and the atrophic thymuses at 40 days and 80 days after irradiation, which were divided into the T type (T) and C type (C) thymus. Bars indicate averages. (B) Flow cytometric analysis of thymocytes from C type thymuses using CD4 and CD8 cell-surface markers. Numbers in quadrants indicate percentage of cells.

γ-irradiation (hereafter these thymic lobes are designated as 40-day and 80-day thymuses, respectively). The earliest time of appearance of fully malignant thymic lymphomas is approximately 100 days after irradiation, and 60% of mice develop lymphomas at 300 days after (5, 16). Clonality was determined in 111 samples of 40-day thymuses and 45 samples of 80-day thymuses by assaying specific V(D)J rearrangements with three primer sets designed for the *TCRβ* locus (16). Figure 1 shows examples, and Supplementary Figs. E1A and B display others. Unirradiated thymus (lane Th) gave six different bands corresponding to possible recombination sites between D and J regions by Dβ1-Jβ1, Dβ2-Jβ2, and Dβ1-Jβ2 probe sets and one band for germline DNA by the former two probe sets. On the other hand, thymic lymphoma DNA (Ly) gave one band only by the Dβ2-Jβ2 probe set used, and brain DNA (Br) gave the germline DNA band by Dβ1-Jβ1 and Dβ2-Jβ2 probe sets. Half (52 of 111) of the 40-day thymuses showed rearrangement patterns identical or similar to that of the control thymus, classified as T type thymus. Most others (43) exhibited only few bands or limited numbers of bands. This group of the thymuses indicated the existence of clonally expanded thymocytes (C type thymus). Several thymuses were classified as C/T type thymus. The fourth group comprised 12 thymuses that exhibited mainly one germline band, probably consisting of immature thymocytes and/or cells other than thymocytes. This study excluded analysis of the G type thymus because of its low incidence. Of the 80-day thymuses, 22 thymuses belonged to T type thymus, and 20 were C type thymus.

Figure 2A shows the thymocyte numbers of 40-day and 80-day thymuses. The average decreased by approximately one seventh in 40-day thymuses, and the decrease tended to be more in C type thymus than in T type thymus. The tendency of decrease was continued in 80-day thymuses. Flow cytometry using CD4 and CD8 cell-surface markers revealed that most thymocytes were DP cells, as normal thymocytes